AD_____

Award Number: DAMD17-03-1-0115

TITLE: Developing Inhibitors of Ovarian Cancer Progression by Targeted Disruption of the Gamma-Synuclein Activated Migratory and Survival Signaling Pathways

PRINCIPAL INVESTIGATOR: Andrew Godwin, Ph.D.

CONTRACTING ORGANIZATION: Fox Chase Cancer Center
Philadelphia, Pennsylvania 19111

REPORT DATE: April 2007

TYPE OF REPORT: Final

PREPARED FOR: U.S. Army Medical Research and Materiel Command
Fort Detrick, Maryland 21702-5012

REPORT DOCUMENTATION PAGE

Form Approved
OMB No. 0704-0188

1. REPORT DATE *(DD-MM-YYYY)*	**2. REPORT TYPE**	**3. DATES COVERED** *(From - To)*
01-04-2007	Final	1 Apr 2003 – 31 Mar 2007

4. TITLE AND SUBTITLE

Developing Inhibitors of Ovarian Cancer Progression by Targeted Disruption of the Gamma-Synuclein Activated Migratory and Survival Signaling Pathways

5a. CONTRACT NUMBER

5b. GRANT NUMBER
DAMD17-03-1-0115

5c. PROGRAM ELEMENT NUMBER

6. AUTHOR(S)

Andrew Godwin, Ph.D.

E-Mail: Andrew.Godwin@fccc.edu

5d. PROJECT NUMBER

5e. TASK NUMBER

5f. WORK UNIT NUMBER

7. PERFORMING ORGANIZATION NAME(S) AND ADDRESS(ES)

Fox Chase Cancer Center
Philadelphia, Pennsylvania 19111

8. PERFORMING ORGANIZATION REPORT NUMBER

9. SPONSORING / MONITORING AGENCY NAME(S) AND ADDRESS(ES)
U.S. Army Medical Research and Materiel Command
Fort Detrick, Maryland 21702-5012

10. SPONSOR/MONITOR'S ACRONYM(S)

11. SPONSOR/MONITOR'S REPORT NUMBER(S)

12. DISTRIBUTION / AVAILABILITY STATEMENT
Approved for Public Release; Distribution Unlimited

13. SUPPLEMENTARY NOTES

14. ABSTRACT

Synucleins are a family of highly **conserved** small proteins that are normally expressed predominantly in **neurons. Very** little is **known** about the physiological functions of **rhe** synucleins. **We have** reported that y-synuclein (also **known** as ***BCSGI)*** is **dramatically** up regulated in the vast majority **(>70%)** of late-stage breast and ovarian cancers (Bruening, **et** al., 2000). **When** overexpressed, ysynuclein significantly stimulates cell proliferation and metastasis **in some** breast **cancer cell** lines. We **have shown** that DNA hypomethylation is a comrnon mechanism underlying the abnormal expression of this gene in tumor cells (Gupta et al., 2003) and hypothesize ***that*** y-synuclein may be a proto-oncogene and that abberant **expression** of this protein may contribute to **the** development **and** progression of **ovarian** cancer. We also found that y-synuclein can promote **cancer** cell survival and inhibit stress- and chemotherapy drug-induced apoptosis by modulating **MAPKs. Specifically,** overexpression **of y-synuclein** lead to constitutive **activation** of **ERK112, and down-regulation *of* JNKl in response** to a host of environmental stress signals, including W, heat shock, sodium **arsenete,** nitric **oxide** and **chemotherapeutic drugs (Pan,** Z-2, **et nl.,** 2002). Because of its high **frequency** of expression in late-stage ovarian cancers, **we** hypothesized that y-synuclein **may** be a promising target for cancer therapy.

15. SUBJECT TERMS
Ovarian cancer, HIV T a t , peptide **drug, yeast two-hybrid assay,** JNK **and** ERK **signaling,** tax01

16. SECURITY CLASSIFICATION OF:			**17. LIMITATION OF ABSTRACT**	**18. NUMBER OF PAGES**	**19a. NAME OF RESPONSIBLE PERSON**
a. REPORT	**b. ABSTRACT**	**c. THIS PAGE**			USAMRMC
U	U	U	UU	33	**19b. TELEPHONE NUMBER** *(include area code)*

Table of Contents

INTRODUCTION:

The synucleins (α, β, γ) are a family of highly conserved small proteins that are normally expressed predominantly in neurons. Little is known about the normal functions of synucleins in physiological conditions. Of the synucleins, α-synuclein is the best characterized because of its potential significance in neurodegenerative diseases including Parkinson's Disease. Previously, we and others have found that γ-synuclein is dramatically up-regulated in the vast majority of late-stage breast (70%) and ovarian (>85%) cancers and that γ-synuclein overexpression can enhance tumorigenicity (Bruening et al., 2000; Ji et al., 1997; Liu et al., 2000). More recent studies have found that γ-synuclein is elevated via epigenetic mechanisms, i.e. promoter hypomethylation, in a broad spectrum of malignancies, including breast, ovarian, lung, and pancreatic, and is emerging as an important protein in cancer metastases (Gupta et al., 2003; Iwaki et al., 2004; Liu et al., 2005). We also found that expression of γ-synuclein induces a phenotype similar to that induced by activation of RhoA/Rac/CDC42, altering the appearance of focal adhesions and stress fibers, and enhancing motility and invasion in ovarian cancer cells (Pan et al, 2006). Other studies have shown that when γ-synuclein is overexpressed in a breast tumor derived cell line, the cells experience a dramatic augmentation in their capacity to metastasize *in vivo* (Jia et al., 1999). Based on these known data, we hypothesize that γ-synuclein may be a proto-oncogene and that abberant expression of this protein may contribute to the progression of ovarian cancer (an now other cancers) and that this tumor-associated protein may be a promising target for drug discovery. We further hypothesize that γ-synuclein may be promoting this phenotype in part by activating the RhoA signal transduction pathway and have shown that RAC as well as the mitogen-activated kinase, ERK1/2, are constitutively activated in cells that overexpress γ-synuclein, but not alpha or beta. Furthermore, we have found that the activation of JNK by stress signals is significantly down-regulated by γ-synuclein, suggesting a role in tumor cell survival and inhibition of apoptosis (Pan et al., 2002). If expression of γ-synuclein in tumor cells induces an invasive phenotype and promotes tumor cell survival, then understanding how γ-synuclein functions may lead to therapies for metastatic disease. Thus, drugs that block the action of γ-synuclein may inhibit the spread of ovarian cancer, as well as other neoplasms. Our studies proposed to further define the function of γ-synuclein through studying the signaling pathways that it affects. We hypothesized that disrupting the interactions between γ-synuclein and its protein binders might provide a means to limit tumor cell metastasis, while inducing limited or no toxicity among other cells in human adults.

BODY

Final Report

In the three previous progress reports we went to great lengths to provide evidence of the work accomplished during the funding period. Overall, we accomplished the majority of the goals set forth in the original application. Nevertheless, γ-synuclein continues to be a fascinating, but difficult protein to unravel functionally.

Task 1. Determine how γ-synuclein modulates JNK and ERK signaling transduction and its effects on cell survival, apoptosis and tumor progression.

As indicated in the previous annual progress report (4-04), we have addressed the objectives of this task as reported in a recent manuscript (Pan, et al., 2006). Briefly, our previous study has shown that exogenous expression of γ-synuclein in breast and ovarian cancer cells leads to increased JNK/ERK activation, cell migration and resistance to apoptosis induced by the microtubule inhibitory drugs (Pan et al., 2002, 2006). In recent studies, we found that γ-synuclein may participate in microtubule regulation (Zhang et al., in preparation, 2007). Like other microtubule-associated proteins, γ-synuclein enhances the

formation of microtubule bundles *in vitro* and alters the phenotype of microtubule bundles induced by MAP2 (Microtubule Associated Protein 2). The presence of synuclein during microtubule polymerization also reduces the microtubule-stability rendered by taxol, which may be linked to the decreased taxol cytotoxicity observed in γ-synuclein-overexpresing ovarian cancer cells. Consistent with these *in vitro* data, we have recently found that exogenously expressed γ-synuclein appears to colocalize with microtubules. Taken together, these new findings suggested a direct linkage between the synuclein and microtubules in cancer.

Task 2. Identify specific mutations or small molecule agents, that specifically disrupt interactions between γ-synuclein and ERK1/2 and between γ-synuclein and JNK, and evaluate them in cell culture models, with a goal of developing them as targeted therapeutics.

As detailed in the previous last two progress reports (4-05, and 4-06), we have identified through two-yeast hybrid assay of a peptide aptamer library (>10 million peptides screened), several small peptides that bind to γ-synuclein and in one case, aptamer 148, interferes with γ-synuclein's ability to bind to other of its protein partners (Cartledge et al., in preparation, 2007). We have also identified additional proteins through a second two-hybrid assay of a *D. melanogaster*-derived cDNA library, which interact with γ-synuclein. We have spent the past 12 months trying to characterize these interactions via pull-downs and co-localization studies, which has proven to be difficult given that γ-synuclein may have many binding partners, none of which are strong interactors. However, several continue to persist as candidate interactors. The significant advancements made since the last progress report is that we have dervived several novel peptide drugs and have shown that they can inhibit tumor cell growth and lead to ovarian tumor cell death *in vitro* (Cartledge et al., in preparation, 2007). Furthermore, we have used reagents generated during the course of these studies, i.e., anti-γ-synuclein antibodies to develop a bead-based immunoassay to evaluate γ-synuclein protein levels in the blood of patients with cancer as a marker for cancer detection.

C- KEY RESEARCH ACCOMPLISHMENTS:

***C.1.* "Developing Inhibitors of Ovarian Cancer Progression by Targeted Disruption of the γ-Synuclein Activated Migratory and Survival Signaling Pathways ".**

1.a. Overexpression of γ-synuclein leads to constitutive activation of ERK and Rho/Rac/Cdc42 and down-regulation of JNK activation in response to stress signals or chemotherapy drugs.

1.b. Overexpression of γ-synuclein induces stress fiber formation and enhances cell migration. Both the basal level and the enhanced cell migration require the activities of both the ERK and Rho/Rac/Cdc42 kinases.

1.c. Overexpression of γ-synuclein may render cancer cells resistant to Taxol and vinblastine by modulating the ERK cell survival pathway and the JNK-mitochondria-Caspase 9/3 apoptotic pathway.

1.d. Identified 53 peptide aptamer clones coding for proteins that demonstrated reproducible interactions with γ-synuclein as assayed.

1.e. Determine that the vast majority of peptide aptamers contain a premature stop codon, suggesting that the N-terminal protion of thioredoxin may interact with γ-synuclein.

1.f. Demonstrated a potential interaction between γ-synuclein and p84N5 (TREX84), a protein that is overexpressed in both breast and ovarian tumors and is essential for the transport of mRNAs from the nucleus to the cytoplasm.

1.g. Initiated a second screen to identify additional interactors of γ-synuclein that can be used to assess the activity of the peptide aptamers.

1.h. Identified three additional putative γ-synuclein-interacting proteins as a result of a yeast two-hybrid screen of a *D. Melanogaster* open reading frame (ORF) library.

1.i. Demonstrated that several peptide sequences that interact with γ-synuclein could partially block interaction of γ-synuclein with several binding partners.

1.j. Modified these peptide sequences by fusing with a portion of HIV (TAT) to create potentially therapeutic agents.

1.k. Performed large-scale purifications of these fusion peptide drugs for assessment *in vitro*.

1.l. Demonstrated that aptamer 148 TAT had cytotoxic activity in ovarian tumor cells.

1.m. Developed a bead-based immunoassay to evaluate γ-synuclein protein levels in the blood of patients with cancer.

1.n. Interaction between 148 TAT and γ-synuclein purified proteins has been demonstrated by *in vitro* co-immunoprecipitation methods.

1.o. Cell Titer-Blue Cell Viability Assay (Promega) was used to assess the cytotoxic effecs demonstrated by the 148 TAT peptide. As measured by this assay, A2780 ovarian tumor cells demonstrated an

additional 30% drop in viability when treated with 148 TAT peptide for 30 minutes as compared to the same cells treated with control TAT peptide alone.

1.p. 148 TAT peptide transduction capability and stability has been measured by western blot analysis. The peptide was found to be stable for 24 hours in A2780 ovarian carcinoma cells, A2780 ovarian carcinoma cells stably overexpressing γ-synuclein, and in two normal right ovarian surface epithelial primary cell lines. The peptide was still detectable in cells at 48 hours although some degradation was apparent in all but the γ-synuclein overexpressing A2780 cells, which retained stable expression of the peptide at this time point.

1.q. Efforts have been made to determine the mode of toxicity of the 148 TAT peptide. Peptide treatment of A2780 cells followed by western blot analysis has demonstrated that cellular death is not due to autophagic or apoptotic mechanisms. The method of toxicity is believed to be physical degradation of cellular components.

1.r. Demonstrated that *in vitro* γ-synuclein can bind the microtubule, induce the formation of microtubule bundles, alter the phenotype of microtubule bundles induced by MAP2 and reduce the stability of microtubules formed in the presence of taxol.

1.s. Demonstrated that γ-synuclein colocalizes with microtubules *in vivo* by confocal microscopy and is associated with cytoskeleton by cell fractionation assay.

1.t. Discovered that exogenous γ-synuclein induces abnormal mitochondria clustering at perinuclear area in A2780 cells.

1.u. Demonstrated that γ-synuclein promotes the formation focal adhesion complex in A2780 cells and OVCAR5 cells when grown on fibronectin by immunoflorescence staining of FAK (focal adhesion kinase).

1.v. Demonstrated that overxpression of γ-synuclein in A2780 cells and OVCAR5 cells leads to enhanced cell adhesion to certain extraxcellular matrix including firbonectin, laminin and vitronectin (but not collagen I and collagen IV) without affecting the expression of cell surface integrin levels.

1.w. Demonstrated that γ-synuclein can specifically bind to phosphatidylinositol phosphates family members but not any other types of lipids *in vitro*.

D- REPORTABLE OUTCOMES:

D.1. "Developing Inhibitors of Ovarian Cancer Progression by Targeted Disruption of the γ-synuclein Activated Migratory and Survival Signaling Pathways",

1.a. Abstracts

Zhong-Zong Pan and A.K. Godwin. γ-Synuclein May Render Cancer Cell Resistance to Paclitaxel by Activating AKT. Proceedings of American Association of Cancer Research, 44:2031, 2003.

Pan, Z.-Z., Vanderhyden, B. and Godwin, A.K. γ-Synuclein transgenic mouse model in cancer initiation and progression. Proceedings of American Association of Cancer Research, 45:5108, 2004.

Guo, G., Farber, M.J., Shiekhattar, R. and Godwin, A.K. Over-expression of death domain containing protein-p84N5 in human ovarian cancer cell lines is associated with cell proliferation. Proceedings of American Association of Cancer Research, 45:1805, 2004. (Selected for an award as an AACR scholar-in-training).

Donna M. Cartledge, Hong Zhang, Ange Kouadio, and Andrew K. Godwin. Small Molecule Agents that Target γ-Synuclein as Novel Therapies for Advanced Stage Breast and Ovarian Cancers. Presented at the 2006 Post Doctoral and Graduate Student Research Symposium, Fox Chase Cancer Center, Philadelphia, PA.

Hong Zhang, Ange Kouadio, Andrew K. Godwin. The Role of γ-Synuclein in Tumor Metastases Presented at the 2006 Post Doctoral and Graduate Student Research Symposium, Fox Chase Cancer Center, Philadelphia, PA.

1.b. Publications

Gupta, A., Godwin, A.K., Vanderveer, L., Lu, A.P., and Liu, J. Hypomethylation of the synuclein γ gene CpG island promotes its aberrant expression in breast carcinoma and ovarian carcinoma. Cancer Res., 63:664-673, 2003. (PMID: 12566312)

Guo, S., Hakimi, M-A., Baillat, D., Chen, X., Farber, M.J., Klein-Szanto, A.J.P., Cooch, N.S., Godwin, A.K., Shiekhattar, R. Linking transcriptional elongation and mRNA export to metastatic breast cancers. Cancer Research, 65:3011-3016, 2005. (S. Guo is under the supervision of Dr. Godwin). (PMID: 15833825)

Pan, Z-Z., Bruening, W., Godwin, A.K. Involvement of RHO GTPases and ERK in synuclein-gamma enhanced cell motility. International Journal of Oncology, 29, 1201-1205, 2006. (PMID: 17016652)

Cartledge, D. and Godwin, A.K. Gamma-synuclein inhibitory TAT peptide causes cytotoxicity in breast and ovarian cancer cells (in preparation, 2007).

Zhang H, Kouadio A, Godwin A.K. Role of synucleins in microtubule organization and stabilization. (in preparation, 2007).

Book chapters and review articles:

Ozols, R.F., Bookman, M., Connolly, D., Daly, M.B., **Godwin**, **A.K**. Schilder, R., Xu, X., Hamilton, T.C. Focus on epithelial ovarian cancer. Cancer Cell, 5:19-24, 2004. (PMID: 14749123)

Pan, Z-Z., **Godwin, A.K**. Oncogenes. Encyclopedia of Molecular Cell Biology and Molecular Medicine. Edited by R.A. Meyers, Second Edition, Volume 9. Wiley-VCH Verlag GmbH & Co. KGaA, Weinheim, pp., 435-495, 2005.

E- CONCLUSIONS:

E.1. "Developing Inhibitors of Ovarian Cancer Progression by Targeted Disruption of the γ-Synuclein Activated Migratory and Survival Signaling Pathways "

In our previous studies, we found that γ-synuclein can interact with two major MAPKs, i.e., ERK and JNK1. Overexpression of γ-synuclein may lead to enhanced activity of ERK and down-regulation of JNK activation in response to stress and chemotherapy drugs. The Rho/Rac/Cdc42 pathway is also activated in cells overexpressing γ-synuclein. Activation of both the Rho/Rac/Cdc42 and the ERK pathways are required for the enhanced cell migration observed in γ-synuclein overexpressing cells. Overexpression of γ-synuclein may render cancer cells resistant to Taxol and vinblastine by modulating the ERK cell survival pathway and the JNK-mitochondria-Caspase 9/3 apoptotic pathway. Taken together, these data continue to indicate that γ-synuclein may have a prominent role in tumorigenesis by enhancing cell motility through modulating the Rho/Rac/Cdc42 and the ERK pathways, and by promoting cell survival and inhibiting apoptosis through modulating the ERK cell survival and the JNK-mitochondria-caspase9/3 apoptotic pathways. Since γ-synuclein is aberrantly expressed in the majority of late-stage ovarian cancers but is not expressed in normal ovarian epithelial cells, γ-synuclein may represent a very promising therapy target for these diseases. In this aspect we have uncovered a number of peptide aptamer sequences that appear to interact with γ-synuclein. Furthermore, we have identified that γ-synuclein may interact with TREX84, an important protein which is overexpressed in breast and ovarian tumors and is involved in mRNA metabolism (Guo et al., 2005). We have made progress in identifying inhibitory γ-synuclein interacting proteins and creating recombinant peptides that are being assessed as novel therapeutics to treat ovarian tumor cell lines which overexpress γ-synuclein. These studies will determine if these peptide drugs lead to disruption of γ-synuclein interactions and effect tumor cell growth *in vitro* and *in vivo*.

F. REFERENCES:

Bruening, W., Giasson, B. I., Klein-Szanto, A. J., Lee, V. M., Trojanowski, J. Q., and Godwin, A. K. Synucleins are expressed in the majority of breast and ovarian carcinomas and in preneoplastic lesions of the ovary. Cancer, *88:* 2154-2163, 2000.

Gupta, A., Godwin, A.K., Vanderveer, L., Lu, A.P., and Liu, J. Hypomethylation of the synuclein γ gene CpG island promotes its aberrant expression in breast carcinoma and ovarian carcinoma. Cancer Res., 63:664-673, 2003.

Iwaki, H., Kageyama, S., Isono, T., Wakabayashi, Y., Okada, Y., Yoshimura, K., Terai, A., Arai, Y., Iwamura, H., Kawakita, M., and Yoshiki, T. Diagnostic potential in bladder cancer of a panel of tumor markers (calreticulin, gamma-synuclein, and catechol-o-methyltransferase) identified by proteomic analysis. Cancer Sci, *95:* 955-961, 2004.Ji, H., Liu, Y. E., Jia, T., Wang, M., Liu, J., Xiao, G., Joseph, B. K., Rosen, C., and Shi, Y. E. Identification of a breast cancer-specific gene, BCSG1, by direct differential cDNA sequencing. Cancer Res, *57:* 759-764, 1997.

Jia, T., Liu, Y. E., Liu, J., and Shi, Y. E. Stimulation of breast cancer invasion and metastasis by synuclein gamma. Cancer Res, *59:* 742-747, 1999.

Liu, H., Liu, W., Wu, Y., Zhou, Y., Xue, R., Luo, C., Wang, L., Zhao, W., Jiang, J. D., and Liu, J. Loss of epigenetic control of synuclein-gamma gene as a molecular indicator of metastasis in a wide range of human cancers. Cancer Res, *65:* 7635-7643, 2005.

Pan, Z. Z., Bruening, W., Giasson, B. I., Lee, V. M., and Godwin, A. K. Gamma-synuclein promotes cancer cell survival and inhibits stress- and chemotherapy drug-induced apoptosis by modulating MAPK pathways. J Biol Chem, *277:* 35050-35060, 2002.

Pan, Z-Z., Bruening, W., Godwin, A.K. Involvement of RHO GTPases and ERK in synuclein-gamma enhanced cell motility. International Journal of Oncology, 29, 1201-1205, 2006.

Ruden, D. M., Ma, J., Li, Y., Wood, K., and Ptashne, M. Generating yeast transcriptional activators containing no yeast protein sequences. Nature, *350:* 250-252, 1991

Surgucheva, I. G., Sivak, J. M., Fini, M. E., Palazzo, R. E., and Surguchov, A. P. Effect of gamma-synuclein overexpression on matrix metalloproteinases in retinoblastoma Y79 cells. Arch Biochem Biophys, *410:* 167-176, 2003.

Wollman, E. E., d'Auriol, L., Rimsky, L., Shaw, A., Jacquot, J. P., Wingfield, P., Graber, P., Dessarps, F., Robin, P., Galibert, F., and et al. Cloning and expression of a cDNA for human thioredoxin. J Biol Chem, *263:* 15506-15512, 1988.

List of Personnel:

Andrew Godwin - Principal Investigator
Srujan Peddapaidi - Summer Assistant I
Donna Cartledge - Graduate Student
Wei Shen - Postdoctoral Associate

Appendices:

Gupta, A., Godwin, A.K., Vanderveer, L., Lu, A.P., and Liu, J. Hypomethylation of the synuclein γ gene CpG island promotes its aberrant expression in breast carcinoma and ovarian carcinoma. Cancer Res., 63:664-673, 2003. (PMID: 12566312)

Guo, S., Hakimi, M-A., Baillat, D., Chen, X., Farber, M.J., Klein-Szanto, A.J.P., Cooch, N.S., Godwin, A.K., Shiekhattar, R. Linking transcriptional elongation and mRNA export to metastatic breast cancers. Cancer Research, 65:3011-3016, 2005. (S. Guo is under the supervision of Dr. Godwin). (PMID: 15833825)

Pan, Z-Z., Bruening, W., Godwin, A.K. Involvement of RHO GTPases and ERK in synuclein-gamma enhanced cell motility. International Journal of Oncology, 29, 1201-1205, 2006. (PMID: 17016652)

[CANCER RESEARCH 63, 664–673, February 1, 2003]

Hypomethylation of the *Synuclein γ* Gene CpG Island Promotes Its Aberrant Expression in Breast Carcinoma and Ovarian Carcinoma[1]

Anu Gupta, Andrew K. Godwin, Lisa Vanderveer, AiPing Lu, and Jingwen Liu[2]

Veterans Affairs Palo Alto Health Care System, Palo Alto, California 94304 [A. G., A. L., J. L.], and Department of Medical Oncology, Fox Chase Cancer Center, Philadelphia, Pennsylvania 19111 [A. K. G., L.V.]

ABSTRACT

Recent studies indicate that *synuclein γ* (*SNCG*) gene, located in chromosome 10, participates in the pathogenesis of the breast and ovary. SNCG, also known as *breast cancer-specific gene 1* (*BCSG1*), is not expressed in normal mammary or ovarian surface epithelial cells but is highly expressed in the vast majority of advanced staged breast and ovarian carcinomas. When overexpressed, *SNCG* significantly stimulates breast cancer proliferation and metastasis. To fully understand the molecular mechanisms underlying the abnormal expression of SNCG in neoplastic diseases, in this study, we extensively examined the methylation status of a CpG island located in exon 1 of *SNCG* gene in a panel of breast and ovarian tumor-derived cell lines to determine whether DNA methylation plays a crucial role in SNCG expression. *In vivo* bisulfite DNA sequencing of genomic DNA isolated from breast cancer cell lines showed that the 15 CpG sites within the CpG island were completely unmethylated in all SNCG-positive cell lines (5 of 5), but were densely and heterogeneously methylated in the majority of SNCG-negative cell lines (3 of 4). The methylation occurred primarily at the CpG sites 2, 5, 7, and 10–15. Similarly, we observed a strong correlation of hypomethylation of the CpG island and SNCG expression in ovarian cancer cell lines (5 of 5). Intriguingly, the methylation pattern in ovarian cancer cells is different from that in breast cancer cells. In SNCG-nonexpressing ovarian cancer cells, all 15 of the CpG sites were completely methylated instead of selective methylation at certain sites shown in breast cancer cells, thereby suggesting a tissue-specific methylation pattern. A correlation between hypomethylation of the exon 1 and expression of SNCG mRNA was also observed in primary breast tumor tissues. The importance of DNA methylation in the control of SNCG expression in cancer cells is further strengthened by demonstration of re-expression of SNCG mRNA in SNCG-negative ovarian and breast cancer cells with a demethylating agent 5-aza-2′-deoxycytidine. In addition, we demonstrate that inhibition of cell growth leads to a decreased mRNA expression and an increased DNA methylation of *SNCG* gene. Taken together, these new findings strongly suggest that DNA hypomethylation is a common mechanism underlying the abnormal expression of this candidate oncogene in breast and ovarian carcinomas.

INTRODUCTION

Recently, methylation of DNA at CpG dinucleotides has been recognized as an important mechanism for regulation of gene expression in mammalian cells. Methylation of cytosines in the CpG sequence located in the promoter region or exon 1 is thought to ensure the silencing of certain tissue-specific genes in nonexpressing cells. Aberrant methylation is now considered an important epigenetic alteration occurring in human cancer. Hypermethylation of normally unmethylated tumor suppressor genes correlates with a loss of expression in cancer cell lines and primary tumors (1–4). On the other hand, failure to repress genes appropriately by abnormal demethylation of tissue-restricted genes or by hypomethylation of proto-oncogenes could result in the loss of tissue specificity and could promote cancer formation (5, 6). Numerous investigations suggest that hypermethylation of promoter CpG islands correlates with transcriptional inhibition in neoplasmas. Most of the hypermethylated CpG islands are located in the promoter region of tumor suppressor genes or DNA repair genes, and DNA methylation is associated with the loss of gene expression in cancer cell lines and primary tumors. However, compared with an extensive list of tumor suppressor genes or cell cycle-regulated genes that are silenced in cancer cells to date, only a few genes have been shown transcriptionally reactivated by DNA demethylation in cancer (7). Although the global hypomethylation in cancers has been observed for several years, it has not received much attention until recently. Initially, hypomethylation of human growth hormone, *α-globin*, and *γ-globin* in cancers was observed by Feinberg and Vogelstein (8). These genes are methylated in normal tissues and become hypomethylated in cancers. Later on, the study was extended to various grades of tumors like benign and malignant colon neoplasmas, and hypomethylation was observed in both types of tumors (9). The hypomethylation and overexpression of proto-oncogenes c-*Myc* and c-*Jun* has been detected in chemically induced tumors in mouse liver (10). Rosty *et al.* (11) has recently reported hypomethylation of *S100A4* gene in pancreatic cell carcinomas. A correlation of hypomethylation and expression of MN/CA9 (a tumor-associated antigen) was reported by Cho *et al.* (12) in renal cell carcinomas. Additionally, DNA hypomethylation and overexpression has been shown for *MDR* in myeloid leukemias (13), *BCL-2* in chronic lymphocytic leukemias (14), *MAGE-1* in melanomas (15), and c-Ha-RAS in gastric carcinomas (10). Recently, Strichman-Almashanu *et al.* (16) have identified unique CpG islands that are methylated specifically in normal tissues and not in cancers.

SNCG,[3] also referred to as the *BCSG1* (*breast cancer specific gene 1*), is a member of a neuronal protein family synuclein and its expression is highly tissue specific (17–21). The SNCG protein is abundantly expressed in the peripheral nervous system such as primary sensory neurons, sympathetic neurons, and motor neurons. However, this tissue specificity was apparently lost during the disease progression of breast cancer and ovarian cancer, because this gene, normally silent in breast tissue and ovary, became abundantly expressed in the vast majority of the advanced staged breast carcinoma and ovarian carcinoma.

The involvement of SNCG in human neoplastic diseases first came to light 5 years ago when SNCG was isolated from a human breast tumor cDNA library and was shown to be overly expressed in infiltrating ductal carcinomas (22). By using *in situ* hybridization, Jia *et al.* demonstrated a stage-specific expression pattern of SNCG mRNA, varying from virtually no detectable expression in normal or benign

Received 4/18/02; accepted 11/26/02.

The costs of publication of this article were defrayed in part by the payment of page charges. This article must therefore be hereby marked *advertisement* in accordance with 18 U.S.C. Section 1734 solely to indicate this fact.

[1] Supported by the Department of Veterans Affairs (Office of Research and Development, Medical Research Service), by a grant from the Ovarian Cancer Research Fund (to A. K. G.), by Grants 1RO1CA83648-01 (to J. L.) and Specialized Programs of Research Excellence (SPORE) P50 CA83638 (to A. K. G.) from National Cancer Institute, and by a Grant (BC010046) from the United States Army Medical Research and Material Command (to J. L.).

[2] To whom requests for reprints should be addressed, at (154P), VA Palo Alto Health Care System, 3801 Miranda Avenue, Palo Alto, CA 94304. Phone: (650) 493-5000, extension 64411; Fax: (650) 849-0251; E-mail: Jingwen.Liu@med.va.gov.

[3] The abbreviations used are: SNCG, synuclein γ; 5-Aza-C, 5-aza-2′-deoxycytidine; FBS, fetal bovine serum; GAPDH, glyceraldehyde-3-phosphate dehydrogenase; HMEC, human mammary epithelial cell; MSP, methylation-specific PCR; OM, oncostatin M; RT, reverse transcription.

breast tissues to low level and partial expression in low-grade ductal carcinoma *in situ* (DCIS) to high expression in advanced infiltrating carcinomas. Immunohistochemical studies to examine SNCG protein expression showed a similar pattern in that it was not detected in normal breast tissues but was detected in a high percentage of stage III/IV breast ductal carcinomas (23). SNCG expression in advanced breast carcinomas is not merely adventitious, but plays a positive role in the process of invasion and metastasis. Our groups and others have demonstrated that exogenous expressions of SNCG induced a more aggressive and invasive phenotype in the breast cancer cell line MDA-MB435 (24), and the inhibition of SNCG with SNCG antisense mRNA reversed the malignant phenotypes of T47D cells (25).

The first piece of evidence suggesting a possible role of SNCG in the development of ovarian carcinoma came from an analysis of the expressed sequence tag database. Lavedan *et al.* (20) noticed that 37% of the human SNCG sequences were originated from an ovarian tumor library, and the rest of the sequences were from brain and breast tumor libraries, thereby predicting that SNCG may also be overexpressed in ovarian tumor. This speculation was confirmed later by Bruening *et al.* (23), who conducted a study to examine SNCG expression in normal ovarian tissue samples and tissues from ovarian carcinoma. This study found that ovarian epithelial cells or ovarian stromal cells from normal ovaries were not stained with anti-SNCG antibody. In contrast, Bruening *et al.* showed that 33 (73%) of 45 ovarian carcinomas strongly reacted with anti-SNCG antibody, and the immunoreactivity was exclusively in malignant ovarian epithelial cells.

To elucidate the mechanisms that underlie the abnormal expression of SNCG in breast cancer cells, a 2.2 kb-fragment of human *SNCG* gene including 1 kb of the 5′-flanking region (−1260 to −170), exon 1 (−169 to +121), and intron 1 (+122 to +935), was isolated in the VA Palo Alto laboratory (26). Our previous studies of SNCG promoter activity in two SNCG-positive and one SNCG-negative breast cancer cell lines suggested that SNCG transcription is primarily controlled by regulatory sequences located in intron 1 and exon 1 but not in the 5′ flanking region.

The intron 1 contains two closely located AP1 recognition sequences. Deletion of these motifs greatly diminished the SNCG promoter activity, suggesting that AP1 is an important transactivator for SNCG transcription in breast cancer cells. Sequence analysis identified a CpG island in exon 1 that contains 15 CpG sites, covering the region −169 to +81, relative to the translation start codon. By using the sodium bisulfite DNA sequencing technique that examined the *in vivo* methylation pattern of the exon 1 region, we found that the CpG sites within the CpG island and its vicinity were partially and heterogeneously methylated in SNCG-negative MCF-7 cells but unmethylated in SNCG-positive SKBR-3 and T47D cells (26).

These initial observations suggest that demethylation of SNCG exon 1 could play a causative role for the expression of SNCG in cell culture. To determine whether demethylation of the exon 1 is a common molecular determinant responsible for the abnormal expression of SNCG in breast carcinoma and ovarian carcinoma, in the present study, we extensively examined the methylation status of exon 1 and SNCG expression in a panel of breast cancer and ovarian cancer cell lines, and in primary breast tumor and normal breast tissues.

Materials and Methods

Cells and Culture Conditions. The breast cancer cell lines, AU565, MCF-7, MDA-MB435, MDA-MB231, MDA-MB 468, T47D, SKBR-3, were cultured in RPMI 1640 with 10% FBS. H3922 was grown in Iscove's modified Dulbecco's medium in the presence of 10% FBS and BT-20 was grown in DME H-16 50% and F-12 50% media supplemented with 10% FBS. The normal mammary epithelial-derived cell line MCF10A was obtained from American Type Culture Collection (ATCC) and cultured according to the instruction provided by ATCC. Two normal human primary mammary epithelial cell lines 184 and 048R with finite life span were cultured in 1:1 mixture of DME/F-12 supplemented with 0.5% FBS, 10 μg/ml insulin, 5 ng/ml epidermal growth factor, 0.1 μg/ml hydrocortisone, and 1 ng/ml cholera toxin. The third finite life span primary cell line derived from the organoid 240L was cultured in complete MEGM medium (Clonetics) supplemented with 10^{-5} M isoproterenol. All HMECs and organoids, and the organoid-derived cell line (240L) were kindly provided by Dr. Martha R. Stampfer at the Lawrence Berkeley National Laboratory, in Berkeley, CA.

The ovarian carcinoma-derived cell lines (A2780 and OVCAR-3, -4, -5, -8) were maintained in DMEM supplemented with 10% FBS, glutamine, and insulin (0.2 IU/ml pork insulin; Novagen; Ref. 27). Human ovarian surface epithelial cell lines were derived as described previously (28). Cells were maintained in a 1:1 mixture of Media 199 and MCDB-105 media, supplemented with 4% FBS and 0.2 IU/ml insulin (29). The life spans of the human ovarian surface epithelial cells (HIO-103, -105, -107, -135) have been extended by ectopically expressing SV40 large T-antigen. These cell lines are nontumorigenic with the exception of HIO-118, which has been shown to form tumors in mice.[4]

Isolation of Genomic DNA from Cell Lines and Tissues. The genomic DNA was isolated from various cell lines by using Promega's wizard DNA isolation kit according to the manufacturer's instructions. Primary breast tumor tissues and normal breast tissues were obtained after surgical resection and stored frozen at −80° C. The tissues were incubated at 55°C in homogenization buffer containing 50 mM Tris (pH 8.0), 1 mM EDTA, 0.5% Tween 20, and 5 mg/ml proteinase K for 3 h, and then genomic DNA was isolated using Promega's DNA isolation kit. Donors of tissue specimens agreed to allow their specimens to be used for research purposes. Breast tumors were staged following standard American Joint Committee on Carcinoma/International Union Against Carcinoma tumor-node-metastasis (TNM) methodology.

Genomic Bisulfite DNA Sequencing. Two μg of genomic DNA from each sample was modified by sodium bisulfite as described previously (2). The modified DNA was amplified with primer SNCG-S2F and SNCG-S2R covering the region −275 to +140. PCR reactions were performed in a volume of 50 μl containing 1× PCR buffer, 1.5 mM $MgCL_2$, 0.2 mM dNTP, 25 pM of each primer, and 2.5 units of platinum Taq polymerase (Life Technology Inc.). PCR reaction was carried out at 94°C for 1 min, and 35 cycles at 94°C for 30 s, 55°C for 30 s, and 72°C for 30 s, and finally 72°C for 5 min. The 415-bp PCR product was gel purified and ligated into PCR2.1 Topo cloning vector (Invitrogen, Carlsbad, CA). After transformation, individual colonies were picked, and the insert was PCR amplified as described above and sequenced using SNCG-S2R as the primer. Table 1 provide the sequences of the oligonucleotide primers used in this study.

RT-PCR Analysis of SNCG mRNA. For cell lines, Ultraspec RNA reagent (Biotecxs Laboratory, Houston, TX) was directly added to the monolayer cell culture grown in culture dishes. For isolation of RNA from tumor tissues, 50–200 mg tissues were homogenized in 2–3 ml of Ultraspec RNA reagent on ice using polytron homogenizer at the setting of 3 with three 10-s bursts. RNA was then isolated from the lysate according to the vendor's protocol. The RT was conducted with random primers (Promega) using Superscript II (Invitrogen). The PCR reaction was carried out at 94°C for 30 s, 60°C for 30 s, and 72°C for 30 s, with initial activation of the enzyme at 94°C for 1 min. Thirty-eight cycles were performed for SNCG and 26 cycles for GAPDH. The PCR was performed using primers SNCG-RT 5′ and SNCG-RT 3′for SNCG and primers GAPDH-RT 5′ and GAPDH-RT 3′ for GAPDH.

Western Blot Analysis. Total cell lysates were isolated from cells as described previously (30). Fifty μg of protein from total cell lysate per sample was separated on 15% SDS PAGE, transferred to nitrocellulose membranes, blotted with goat anti-SNCG polyclonal antibody (E-20, sc-10698; Santa Cruz Biotechnology) at 1:200 dilution using an enhanced chemiluminescence (ECL) detection system (Amersham). Membranes were stripped and reblotted with anti-β-actin monoclonal antibiotic (Sigma) to normalize the amount of protein loaded on gels.

MSP. Two μg of genomic DNA isolated from ovarian cell lines was treated with sodium bisulfite and purified using Promega's DNA clean-up kit.

[4] A. K. Godwin, unpublished observations.

Table 1 *Sequences of SNCG gene-specific primers*

Primer	Nucleotide sequence (5′ to 3′)
RT-PCR primers	
SNCG-RT 5′	CAAGAAGGGCTTCTCCATCGCCAAGG
SNCG-RT 3′	CCTCTTTCTCTTTGGATGCCACACCC
GAPDH-RT 5′	CCATCACTGCCACCCAGAAGAC
GAPDH-RT 3′	GGCAGGTTTTTCTAGACGGCAG
Bisulfite sequencing PCR primers	
SNCG-S2F	GGTTGAGTTAGTAGGAGTTTA
SNCG-S2R	CCTACCATACCCCACTTACCC
MSP primers	
SNCG-U1CF	GGTTTTTGTATTAATATTTTATTGGTG
SNCG-U2R	ACAAAACTAAATCTCCCTACAAACTACAA
SNCG-M1F	TCGTATTAATATTTTATCGGCGT
SNCG-M2R	ACGAAACTAAATCTCCCTACGAACTACGT
SNCG-WF	ACGCAGGGCTGGCTGGGCTCCA
SNCG-WR	CCTGCTTGGTCTTTTCCACC

The treated DNA was dissolved in 20 μl of water, and 2 μl was used for MSP. The primers specific for unmethylated DNA were SNCG-U1CF and SNCG-U2R; the primers for methylated DNA were SNCG-M1F and SNCG-M2R. These two sets of primers were designed to amplify the same region of exon 1 from −139 to −37, covering the CpG sites 2–11 and yielding a product of 102 bp. The PCR conditions for both sets of primers were as follows: first cycle at 94°C for 1 min to activate the hot start enzyme, then 30 cycles of 94°C for 30 s, 52°C for 30 s, and 72°C for 30 s, and a final elongation at 72°C for 5 min.

5-Aza-C Treatment. The SNCG-negative breast cancer cell lines (MCF-7 and MDA-MB435) and ovarian cell lines (HIO-135, OVCAR4, and OVCAR8) were cultured in medium containing 0, 1, 5, or 10 μM of 5-Aza-C for 6 days. The medium and drug were replaced every 24 h.

Stable Transfection of MCF-7 Cell Line. MCF-7 cells were transfected with pCIneo vector alone (mock transfected) or with pCIneo-SNCG, and the pooled transfectants were selected by adding 300 μg/ml of G418. The expression of SNCG was confirmed by Western blotting and the cells were further used for proliferation assays.

Proliferation Assay. For HMEC-184, 1.2×10^4 cells were seeded in 24-well plate and treated with 50 ng/ml of OM for 1 and 3 days. [^{3}H]thymidine incorporation was done as described previously (31). For mock- and SNCG-transfected MCF-7 cells, 1×10^3 cells were seeded in black 96-well plates in RPMI medium containing 10% FBS and were harvested at indicated intervals of time. The total DNA content was estimated using cyquant cell proliferation assay kit (Molecular Probes) as per the manufacturer's instructions.

Flow Cytometry Analysis. MCF7-SNCG or MCF7-neo cells were seeded at a density of 2×10^5 in 100-mm dishes in RPMI containing 10% serum. After 24 h, the medium was replaced with RPMI having 0.5% serum. The cells were harvested after 48 h, and DNA content was analyzed as described earlier (32).

Statistical Analysis. Comparisons of experimental data were analyzed by a two-tailed Student's *t* test. A $P < 0.05$ was considered to indicate a statistically significant difference.

RESULTS

Examination of SNCG mRNA Expression in Malignant and Normal Mammary Epithelial Cell Lines. Total RNA was isolated from 10 breast cancer cell lines, and RT-PCR was conducted using specific primers for SNCG and a housekeeping gene, *GAPDH*. SNCG mRNA was detected in 6 of 10 cell lines including AU565, BT-20, SKBR-3, T47D, H3922, and MDA-MB231 (Fig. 1*A*, and data not shown). The remaining four cell lines either showed no expression of SNCG mRNA such as MCF-7, H3396, and MDA-MB435 or expressed this gene at a very low level (Fig. 1*A*, *MDA-MB468*). In contrast, RT-PCR detected equal expression of GAPDH mRNA in all of the cell lines. Western blot analysis (Fig. 1*B*), using specific anti-SNCG antibody, demonstrated SNCG protein expression in the same six cell lines that express the mRNA but not in the four cell lines that express no mRNA or a trace amount, thereby providing a solid validation for the results of the RT-PCR.

We further examined SNCG mRNA and protein expression in one normal mammary epithelium-derived cell line, MCF10A, and 2 primary normal HMEC lines, HMEC-184 and HMEC-048R. Unlike MCF10A cells that can grow in culture indefinitely, the HMEC lines have limited life span. Fig. 1*C* shows that MCF10A expressed a trace amount of SNCG mRNA, as detected by RT-PCR, but SNCG protein could not be detected by immunoblotting. Unexpectedly, both of the HMEC cells showed reasonable levels of SNCG mRNA and protein, which contradicted previous studies by *in situ* hybridization and Western blot that neither detected the mRNA or the protein of SNCG using normal human breast tissues, suggesting that culturing *in vitro* may induce *SNCG* gene expression

Methylation Status of SNCG Exon 1 in Malignant and Normal Mammary Epithelial Cell Lines. To identify the correlation between DNA methylation of exon 1 and expression of SNCG, we examined the *in vivo* methylation status of all of the cell lines by genomic bisulfite sequencing. Genomic DNAs were treated with sodium bisulfite, and the modified DNAs were amplified with the primer SNCG-S2F and SNCG-S2R. This primer set specifically amplified the modified sense strand of *SNCG* gene from −275 to +140, covering the entire exon 1 and its vicinity. The results obtained from 12 cell lines are summarized and are shown schematically in Fig. 2.

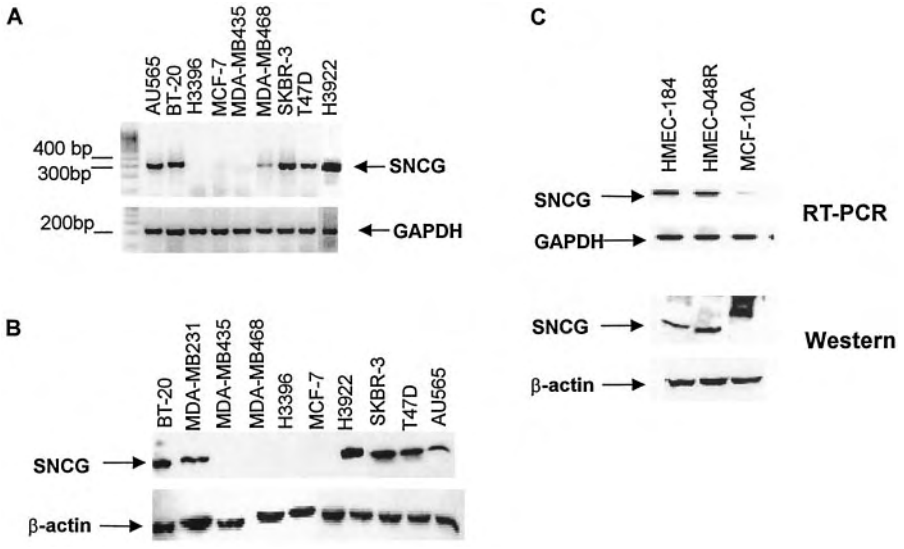

Fig. 1. SNCG expression in breast cancer cell lines and normal HMEC lines. *A*, SNCG mRNA expression in 10 breast cancer cell lines was examined by RT-PCR analysis. One μg of total RNA was used in the reaction of RT in a volume of 20 μl. Two μl of the RT product was used in PCR with specific primers to SNCG or GAPDH. The RT-PCR products were separated on a 1.5% agarose gel and stained with ethidium bromide. *B*, SNCG protein expression in the same cancer cell lines was examined by Western blot by using 20 μg of protein of total cell lysate. *C*, SNCG expression in two finite life-span HMECs (184 and 048R) and one immortalized HMEC line (MCF10A) was examined by RT-PCR (*top panel*) and Western blot (*bottom panel*) as described in *A* and *B*.

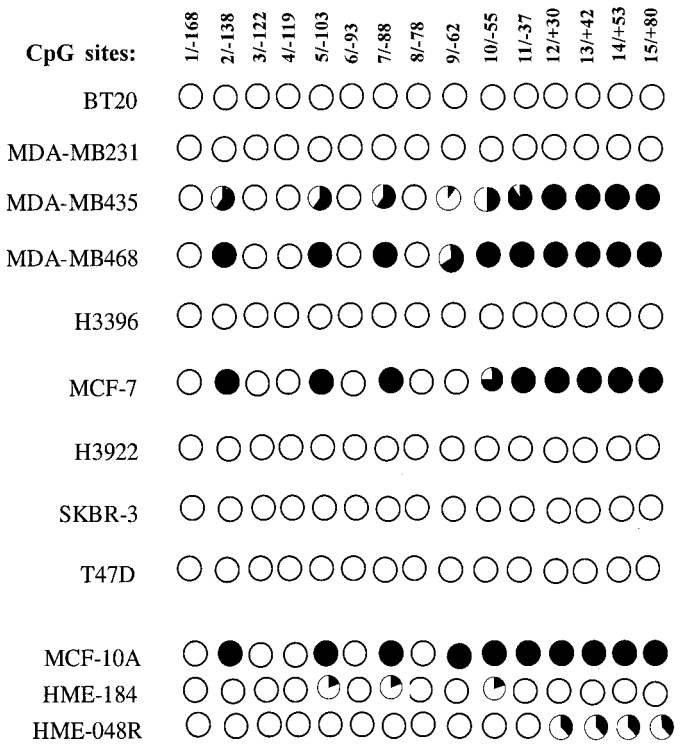

Fig. 2. Methylation status of CpG island in SNCG exon 1 region in various breast cancer cell lines. Genomic DNA was isolated from different cell lines and was modified by sodium bisulfite. Primers SNCG-S2F and SNCG-S2R were used to amplify the region −275 to +140 of modified sense strand of SNCG. CpG positions are indicated relative to the translation start codon, and each circle in the figure represents a single CpG site. For each cell line, the percentage methylation at a single CpG site is calculated from the sequencing results of 6–8 independent clones. ●, 100% methylation; ○, 0% methylation.

The data demonstrated a specific and consistent pattern of methylation in four of five SNCG-negative cell lines. In MCF10A cells, the CpG sites, 2, 5, 7, and 10–15 CpG, were consistently methylated, a pattern identical to the other three cancer cell lines (MDA-MB435, MDA-MB468, and MCF-7). In contrast to SNCG-negative cells, all SNCG-positive cell lines contain unmethylated exon 1. H3396 is the only cell line that has unmethylated CpG island but did not express the *SNCG* gene. In this cell line, repression of transcription by other factors such as lack of transcriptional activator or expression of repressor, may contribute to the loss of SNCG expression despite promoter demethylation. Nevertheless, the results presented in Figs. 1 and 2 clearly demonstrate that the silencing of SNCG expression in mammary epithelial cell lines is correlated predominantly with methylation of exon 1 at specific CpG sites regardless of whether they were originated from breast tumor or from normal breast tissue.

Examination of SNCG mRNA Expression and the Status of Exon 1 Methylation in Primary Breast Tumors. Because the above data confirmed a role of demethylation in *SNCG* gene expression in breast cancer cells in culture, we wanted to know whether the demethylation-dependent gene expression occurs under *in vivo* conditions as well. First, using RT-PCR assays, we examined SNCG mRNA expression in 10 breast tumors, most of which were diagnosed as invasive ductal carcinoma with histological grade of II and above. The pathological characteristics of the tumor samples are listed in Table 2. The expression level of SNCG mRNA in the tumor-adjacent normal tissue from each patient was also determined. In this experiment, T47D cells were used as a positive control. Fig. 3. *top panel*, show the results of RT-PCR and the *next panel down* presents the relative SNCG mRNA levels after normalization with the signal of GAPDH. These results demonstrate that of 10 patient samples, 9 patients displayed SNCG expression in tumor samples. SNCG mRNA was not detected in five tumor-adjacent normal tissues (N1, N5, N7, N8, and N10), whereas low levels were detected in other four normal samples (N2, N3, N6, and N9), and a high level was found in N4. The detection of SNCG expression in the five tissue samples, supposed to be normal, prompted us to reexamine the original tissue slices; we found that all of the adjacent "normal" tissues contained regions of infiltrating tumor cells, which were the likely source of SNCG mRNA detected in these tissue samples.

Second, to determine whether the expression of SNCG in breast tumors is associated with hypomethylation, we selected five patient samples of both tumor and normal tissues for genomic bisulfite sequencing. The sequencing results are summarized in Table 3. The N/T pair number 7, which were SNCG-negative for both the normal tissue and the tumor, showed methylation in five of five clones for normal tissue and four of six clones for tumor. Importantly, the methylation occurred at the CpG sites 2, 5, 7, and 10–15, exactly matching the methylation pattern seen in cell lines. The N/T pair number 8, in which the normal tissue did not show any expression and the tumor showed low level of SNCG mRNA, the exon 1 was methylated in all of the clones from the normal tissue and was partially demethylated in the tumor tissue. In N/T pair number 6, the exon 1 was unmethylated for both normal and tumor tissues, which correlated well with the SNCG expression. In N/T pairs numbers 1 and 5, the exon 1 was unmethylated in tumors as well as in normal tissues, albeit with a lack of SNCG expression in normal tissues, suggesting that demethylation could occur before the gene expression. Taken together, the results from breast tumor tissues agreed to a large extent with the results from breast cancer cell lines and provided critical *in vivo* evidence to support the role of DNA methylation in the control of SNCG expression.

Table 2 *Characteristics of surgical breast tumor specimens*

The tumors were staged following standard American Joint Committee on Carcinoma/International Union against Carcinoma tumor-node-metastasis methodology. The SNCG mRNA expression was determined by RT-PCR and normalized with the mRNA levels of GAPDH as shown in Fig. 3. The double ++ sign indicates the ratio of SNCG mRNA:GAPDH mRNA > 1, the single + sign indicates a ratio of SNCG mRNA:GAPDH mRNA > 0.25, and the − sign indicates a ratio of SNCG mRNA:GAPDH mRNA < 0.2.

Tumor sample no.	Diagnosis	Histologic grade	Nuclear grade	Tumor cells positive axillary lymph nodes	ER	SNCG mRNA expression
T1	Infiltrating (95%) and *in-situ* carcinoma	III	na[a]	34/38	na	++
T2	*In-situ* and invasion duct carcinoma	na	na	11/15	na	++
T3	*In-situ* and infiltrating duct carcinoma	III	na	15/26	+	+
T4	*In-situ* and invasion duct carcinoma	III	III	0/22	−	+
T5	*In-situ* and invasion duct carcinoma	III	na	2/12	na	++
T6	*In-situ* and invasion duct carcinoma	III	III	7/18	+	++
T7	Invasive carcinoma, ductal type	III	III	0/13	na	−
T8	Invasive ductal carcinoma	II/III	II/III	na	−	−/+
T9	*In-situ* and invasive lobular carcinoma	II/III	II/III	7/16	+	+
T10	Invasive ductal carcinoma	III	III	5/18	na	+

[a] na, the information was not available; ER, estrogen receptor.

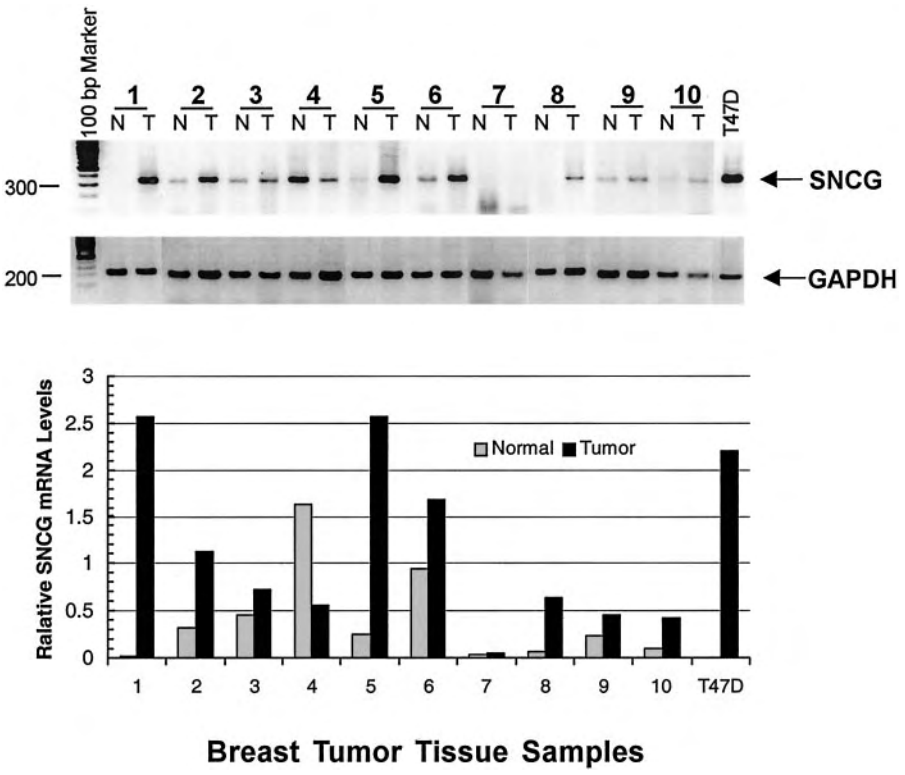

Fig. 3. Detection of SNCG mRNA and GAPDH mRNA in primary breast tumors and in matched normal breast tissue adjacent to tumors. RNA was isolated from 10 pairs of primary breast tissues; *T*, tumor tissue; *N*, normal breast adjacent to tumor. The PCR products were visualized on 1.5% agarose gels stained with ethidium bromide (*top panel*). The intensity of PCR product was scanned by Bio-Rad Fluro-S MultiImager system and quantified by the program of Quantity One. The relative SNCG mRNA levels are presented as the ratio of SNCG mRNA:GAPDH mRNA. SNCG-positive cell line T47D was used in this experiment as a positive control. The data shown are representative of two to three separate RT-PCRs.

Comparison of SNCG mRNA Expression and the Methylation Status of Exon 1 in Normal Breast Tissues with Invasive Breast Carcinomas. It is possible that SNCG mRNA detected in the tumor-adjacent normal tissues was produced by infiltrated tumor cells instead of normal cells. Alternatively, the genetic background of noncancerous tissue adjacent to the tumor cells has been changed, which could activate SNCG expression. We evaluated these possibilities by an examination of SNCG expression in 10 invasive tumors and in 6 normal breast tissues obtained from reduction mammoplasty of healthy individuals. RT-PCR analysis showed that of 10 tumor tissues, 8 displayed high expression of SNCG (Fig. 4*A*, *left panel*). In contrast, under the same conditions, RT-PCR did not detect SNCG expression in normal samples (Fig. 4*A*, *right panel*). The bisulfite genomic sequencing was done for five tumors and the results showed that all of the tumor samples contained mostly unmethylated *SNCG* gene, whereas the normal breast tissues contained methylated as well as unmethylated *SNCG* gene. The percentage methylation for normal breast and tumor samples is presented in Fig. 4*B*, and the difference in methylation was found to be statistically highly significant. ($P \leq 0.003$). Because the majority of genetic materials from normal breast tissue were derived from fat cells and fibroblasts, and only a small portion was actually from the epithelium, it is possible that the unmethylated allele belonged to other cell types.

We further extended our study to organoids. They were epithelial clumps obtained by digestion of normal breast tissue from one donor with collagenase and hyaluronidase at 37°C for 24–72 h. Fig. 5 showed the results of RT-PCR from the organoids before and after extensive cell culture to become finite HMECs. Whereas a very low level of SNCG mRNA was detected in the organoids in which epithelial cells were incubated in culture medium containing growth factors for only 24–72 h, a high level of SNCG mRNA was shown in the matching HMECs. Sequencing results showed that the organoids contained mostly methylated clones (75%) but the finite life span HMECs were completely unmethylated. These data combined with Fig. 1*C* suggest that SNCG is not expressed *in vivo* in normal mammary epithelial cells, however, during the initial selection and culturing *in vitro*, the *SNCG* gene expression is induced through demethylation by growth factors present in the culture medium. SNCG expression may stimulate these primary cultures of cells to proliferate.

To further study that SNCG expression, controlled by demethylation, contributes to the cell proliferation, a normal mammary epithelial cell line HMEC-184 was treated with cytokine OM, which has been previously shown to inhibit the proliferation of HMECs (31). Cells were treated with OM at a concentration of 50 ng/ml for the indicated intervals of time, and cell proliferation was determined by [^{3}H]thymidine incorporation assay. Fig. 6*A* shows that OM treatment led to 30% inhibition of cell growth after 1 day of treatment, whereas up to 60% of inhibition was observed after 3 days of treatment. RT-PCR analysis (Fig. 6*B*) showed that levels of SNCG expression in OM-treated cells was concomitantly reduced by 70% as compared with control. With bisulfite genomic sequencing, four of six clones were found to be methylated in OM-treated cells, whereas all five of the clones sequenced from the untreated cells were unmethylated.

Table 3 *Bisulfite sequencing of cloned PCR products from breast tumor specimens*

DNA was isolated from five pairs of primary breast tissues in which T represents tumor tissue and N represents normal breast tissue adjacent to tumor. Genomic bisulfite sequencing of the exon 1 region of SNCG was performed as described in the "Materials and Methods" section. Four to eight clones from each tissue sample were sequenced. The expression of SNCG mRNA was determined and described in Fig. 3.

Breast tissue samples	Total no. of clones sequenced	Exon 1 methylated	Exon 1 unmethylated	SNCG RT-PCR
N1	8	0	8	−
T1	8	1	7	++
N5	9	0	9	−
T5	7	1	6	++
N6	8	0	8	+
T6	8	1	7	+
N7	5	5	0	−
T7	6	4	2	−
N8	4	4	0	−
T8	8	6	2	−/+

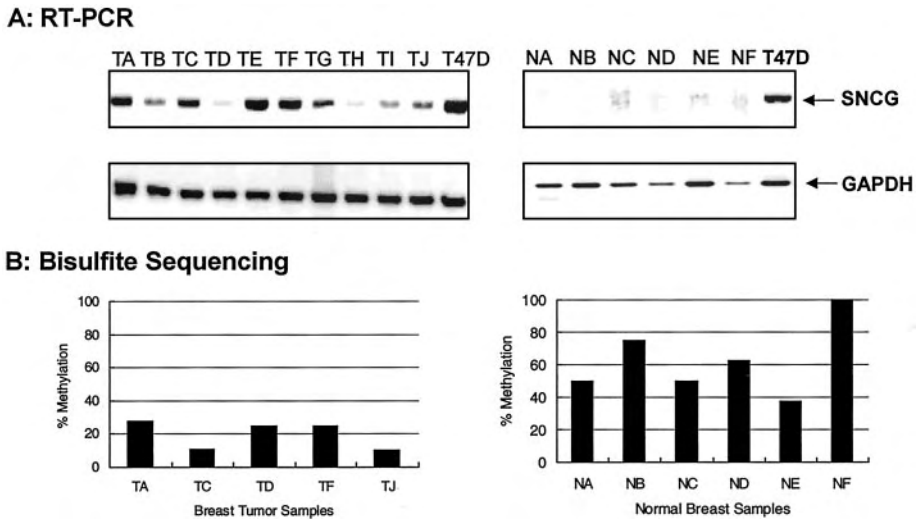

Fig. 4. RT-PCR analysis of SNCG mRNA expression in breast tissue samples from healthy individuals and from patients with advanced breast carcinomas. *A*, six normal breast tissues *NA–NF* (*right panel*) were obtained from healthy donors after mammoplasty, and RNA was isolated from 300–400 mg of tissue per sample. RNA form 10 tumor tissues of advanced breast carcinomas *TA–TJ* (*left panel*) was also isolated. RT-PCR to detect SNCG and GAPDH mRNA was conducted. RNA of T47D cells was used as a positive control. *B*, DNA was isolated from six normal breast tissues (*NA–NF*) and five tumors (*TA, TC, TD, TF, TJ*). Genomic bisulfite sequencing of the exon 1 region of SNCG was performed for 6–8 clones per sample as described in the "Materials and Methods" section. The *bar diagram*, the percentage of methylated clones. The difference in the degree of methylation between normal samples and tumor samples was evaluated using two-tailed Student's *t* test. Statistically significant difference ($P = 0.003$) between normal and tumor samples was reached.

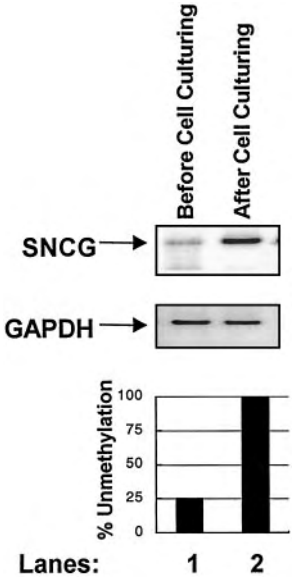

Fig. 5. Expression of SNCG in organoid before and after culturing. RNA and DNA were isolated from organoids (240L) obtained from normal breast tissue of one donor after mammoplasty (*Lane 1*) and the matching HMECs that were developed from the same organoids after continuous culturing (*Lane 2*). RT-PCR to detect SNCG and GAPDH mRNA was conducted as described earlier. The *bar diagram* (*bottom panel*), the percentage of unmethylated clones after genomic sulfite sequencing.

To directly examine the relationship between SNCG expression and cellular proliferation, SNCG was stably transfected into MCF-7 cells, and pool population was selected for both mock- and SNCG-transfected cells. Western blot detected an abundant amount of SNCG protein in MCF7-SNCG transfectants (Fig. 7*A*). The proliferation rate of MCF7-SNCG was compared with mock-transfected MCF-7 cells by using Cyquant cell proliferation assay kit. Fig. 7*B* shows that SNCG-transfected cells proliferate faster than mock-transfected cells, and a >2-fold increase in cell proliferation was observed after 5 days. Cell cycle analysis (Fig. 7*B*, *inset*) showed that SNCG-transfected cells have more cells in S phase (33.11 + 3.2 in SNCG-transfected cells compared with 22.4 + 2.3 in mock-transfected cells) and less in G_2-M (15.06 + 2.8) compared with mock-transfected cells (22.22 + 1.5). Overall, these data suggest that SNCG is a stimulating factor for cell proliferation; the SNCG expression is correlated with demethylation of the exon 1 and that the inhibition of cell growth leads to an increased DNA methylation at the CpG island of the *SNCG* gene, resulting in reduced expression.

Examination of SNCG mRNA Expression in Malignant and Normal Ovarian Epithelium-derived Cell Lines. To determine whether demethylation of exon 1 is also a causal factor for SNCG expression in ovarian cancer cells, the experiments of RT-PCR and *in vivo* genomic sequencing were conducted in five ovarian tumor-derived cell lines and five normal ovarian epithelium-derived cell lines (HIOs). The results of RT-PCR are presented in Fig. 8, *upper panel*, and the summarized sequencing data are shown in Fig. 9. Among the five cancer cell lines, OVCAR3 and OVCAR5 expressed high levels of SNCG mRNA, and these cells contained fully demethylated exon 1, whereas A2780 expressed a moderate level of SNCG mRNA, and exon 1 in these cells was partially methylated. In

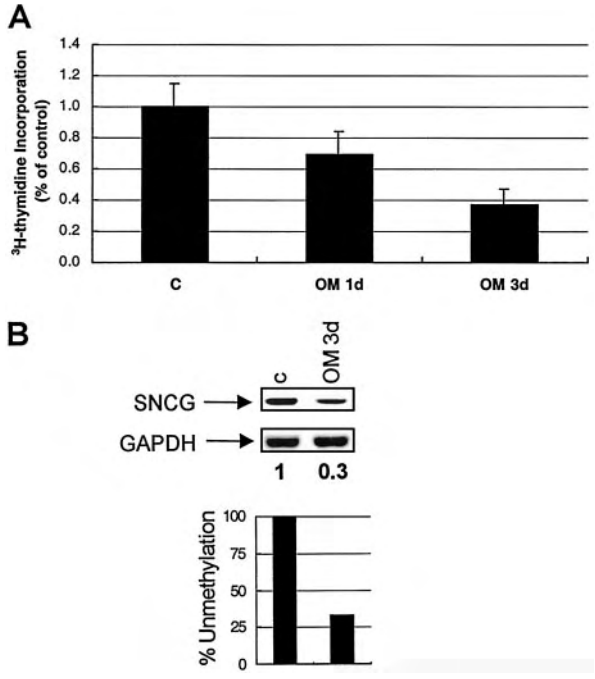

Fig. 6. Regulation of cell proliferation and SNCG mRNA expression and DNA methylation in HMEC-184 by OM. *A*, 1.2×10^4 cells were seeded in 24-well plate and treated with 50 ng/ml for 1 and 3 days. Cells were then pulsed with [^{3}H]thymidine for 16 h. The amount of radioactivity incorporated was determined by trichloracetic acid precipitation. *B*, mRNA expression and DNA methylation of SNCG in HMEC-184 by RT-PCR analysis and DNA bisulfite sequencing. Equal numbers of cells were seeded in 100-mm dishes for control and OM treatment of 3 days. The cells were then harvested for RNA and DNA isolation. The *bar diagram* (*bottom panel*), the percentage of unmethylated clones after genomic sulfite sequencing.

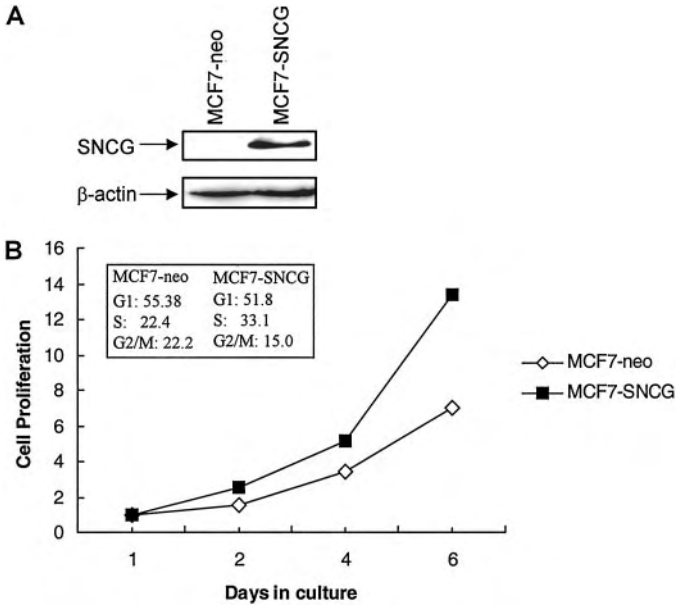

Fig. 7. Cell proliferation assay and cell cycle distribution of DNA in mock- and SNCG-transfected cells. *A*, MCF-7 was transfected with the pCIneo vector or with pCI-SNCG, and the pool populations were selected with 300 μg/ml G418. SNCG protein expression in the mock- and SNCG-transfected pool population of MCF-7 was examined by Western blot by using 20 μg of protein of total cell lysate. *B*, 1000 cells were seeded per well in black 96-well plates for each cell type and harvested at indicated intervals of time. The total DNA content was estimated using fluorescent dye as described in "Materials and Methods." The proliferation rate is expressed as the fold of DNA content in day 1 of each cell population. The data presented are derived from three separate experiments in which quadruplicate wells were used in each condition. The proliferation assay was also carried out in medium containing a different amount of FBS, and the proliferation rates of MCF7-SNCG cells were consistently higher than MCF7-neo cells in all of the assays. *Inset*, for cell cycle analysis, 2×10^5 cells were seeded in 100-mm dishes in RPMI containing 10% media. Next day, the cells were washed with PBS, and RPMI containing 0.5% of medium was added to the cells. After 48 h, the cells were harvested and analyzed by flow cytometry.

contrast, OVCAR4 and OVCAR8 did not express SNCG mRNA at all, and all of the 15 CpG sites of the CpG island in these two cell lines were completely methylated. Thus, SNCG expression appears to correlate very well with the demethylation of *SNCG* gene in ovarian cancer cell lines. Interestingly, the methylation pattern in ovarian cancer cells is different from that in breast cancer cells. The specific methylation patterns of ovarian cancer cell lines and breast cancer cell lines are presented in Table 4. Among the five normal HIO cell lines, SNCG mRNA was detected only in HIO-107 cells. Within eight clones of HIO-107 that were sequenced, four clones were completely methylated at every CpG site of CpG island, whereas the four other clones were nearly unmethylated. Other HIO lines showed no expression of SNCG mRNA, although all four of the cell lines displayed demethylation of the CpG island to a different extent. Thus, these data suggest that in normal ovarian epithelium-derived cell lines, besides DNA methylation, there are other factors that repress SNCG expression. Because all of the CpG sites in the CpG island of SNCG in ovarian cancer cells were methylated in SNCG-negative cells and unmethylated in SNCG-positive cells, it is possible to determine the methylation status by using a MSP assay. To explore this possibility, the bisulfite-modified genomic DNAs were amplified with the methylation-specific primers SNCG-M1F or SNCG-M2R, or the primers corresponding to unmethylated sequence, SNCG-U1CF and SNCG-U2R (Table 1). The *bottom panel* of Fig. 8 shows that a strong band of 102 bp (*SNCG-M*), corresponding to methylated sequence of exon 1 (−139 to −37), was amplified with the methylated primers from SNCG-negative OVCAR4 and OVCAR8 cells, but this band was not amplified from SNCG-positive OVCAR3 and OVCAR5 cells. In contrast to the methylated primers, the same region was specifically amplified using unmethylated primers from OVCAR3 and OVCAR5 but was not amplified from OVCAR4 and OVCAR8. MSP detected both methylated and unmethylated alleles from A2780. Thus, the MSP produced similar results as the direct sequencing. Likewise, the results of MSP of five HIO cell lines agreed to a large degree with the sequencing data and showed that HIO-107 and HIO-108 contained unmethylated and methylated alleles and HIO-103 and -105 contained mostly unmethylated alleles, whereas HIO-135 contained mainly methylated *SNCG* gene. These data suggest that MSP can reliably

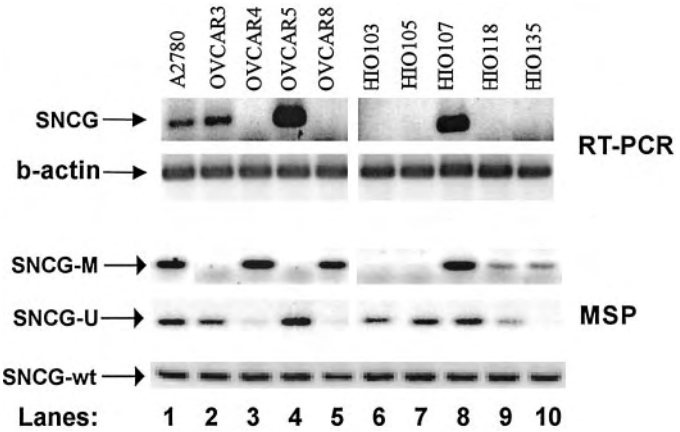

Fig. 8. Detection of SNCG mRNA in ovarian cancer and normal ovarian epithelium-derived (HIO) cell lines by RT-PCR analysis and the methylation status of exon 1 by MSP. *A*, the ovarian cancer and HIO cells were analyzed for SNCG mRNA and β-actin mRNA. *B*, MSP was used to assess the methylation status of SNCG CpG islands in each cell lines. Bisulfite-modified genomic DNA was used as template to amply exon 1 region −139 to −37. The PCR reactions with primers to detect methylated DNA and unmethylated DNA were performed separately. *SNCG-M*, methylated primers; *SNCG-U*, unmethylated primers; *SNCG-wt*, primers corresponding to the wild-type sequence of unmodified DNA The unmodified genomic DNA was amplified with primers corresponding to the wild-type sequence as a positive control for the quality of DNA.

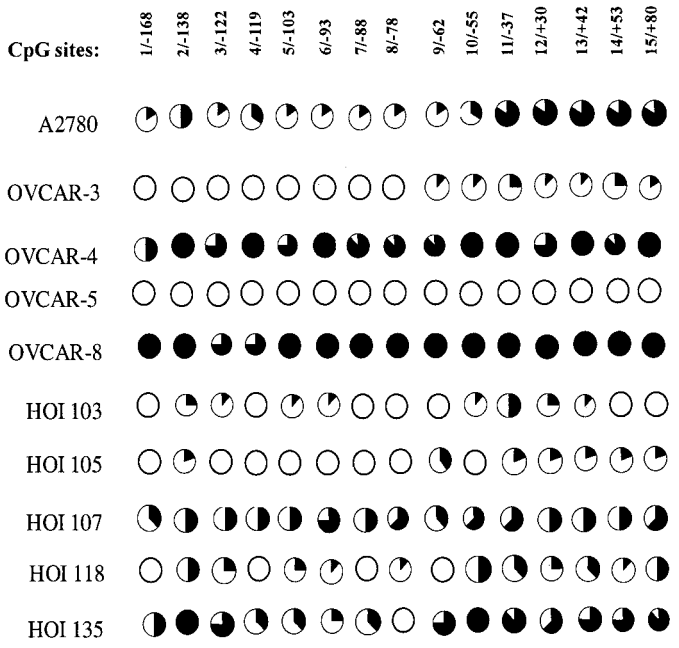

Fig. 9. Methylation status of CpG islands in SNCG exon 1 region in various ovarian cancer and HIO cell lines. CpG positions are indicated relative to the translation start codon, and *each circle* in the figure represents a single CpG site. For each cell line, the percentage methylation at a single CpG site is calculated from the sequencing results of 6–8 independent clones. ●, 100% methylation; ○, 0% methylation.

Table 4 *Comparison of methylation patterns of breast epithelium-derived cells with ovarian epithelium-derived cell lines*

	CpG position														
	1/−168	2/−138	3/−122	4/−119	5/−103	6/−93	7/−88	8/−78	9/−62	10/−55	11/−37	12/+30	13/+42	14/+53	15/+80
MDA-MB468	−	+	−	−	+	−	+	−	−	+	+	+	+	+	+
	−	+	−	−	+	−	+	−	−	+	+	+	+	+	+
	−	+	−	−	+	−	+	−	+	+	+	+	+	+	+
	−	+	−	−	+	−	+	−	+	+	+	+	+	+	+
	−	+	−	−	+	−	+	−	+	+	+	+	+	+	+
	−	+	−	−	+	−	+	−	+	+	+	+	+	+	+
	0	100	0	0	100	0	100	0	66.7	100	100	100	100	100	100% methylation
MCF10A	−	+	−	−	+	−	+	−	−	+	+	+	+	+	+
	−	+	−	−	+	−	+	−	−	+	+	+	+	+	+
	−	+	−	−	+	−	+	−	−	+	+	+	+	+	+
	−	+	−	−	+	−	+	−	−	+	+	+	+	+	+
	−	+	−	−	+	−	+	−	−	+	+	+	+	+	+
	−	+	−	−	+	−	+	−	−	+	+	+	+	+	+
	−	+	−	−	+	−	+	−	−	+	+	+	+	+	+
	−	+	−	−	+	−	+	−	−	+	+	+	+	+	+
	0	100	0	0	100	0	100	0	0	100	100	100	100	100	100% methylation
OVCAR-4	+	+	+	+	+	+	+	+	+	+	+	+	+	+	+
	+	+	+	+	+	+	+	+	+	+	+	+	+	+	+
	+	+	+	+	+	+	+	+	+	+	+	+	+	+	+
	−	+	+	+	+	+	+	+	+	+	+	+	+	+	+
	−	+	+	+	−	+	−	+	+	+	+	+	+	+	+
	−	+	+	+	+	+	+	+	+	+	+	+	+	+	+
	−	+	−	+	−	+	+	−	−	+	+	−	+	−	+
	+	+	−	+	+	+	+	+	+	+	−	+	+	+	+
	50	100	75	100	75	100	87.5	87.5	87.5	100	87.5	87.5	100	87.5	100% methylation
OVCAR-8	+	+	+	+	+	+	+	+	+	+	+	+	+	+	+
	+	+	+	+	+	+	+	+	+	+	+	+	+	+	+
	+	+	+	+	+	+	+	+	+	+	+	+	+	+	+
	+	+	+	+	+	+	+	+	+	+	+	+	+	+	+
	+	+	+	+	+	+	+	+	+	+	+	+	+	+	+
	+	+	+	−	+	+	+	+	+	+	+	+	+	+	+
	+	+	−	+	+	+	+	+	+	+	+	+	+	+	+
	+	+	−	+	+	+	+	+	+	+	+	+	+	+	+
	100	100	75	87.5	100	100	100	100	100	100	100	100	100	100	100% methylation

distinguish the unmethylated *SNCG* from the methylated gene in ovarian cancer cells.

Reexpression of SNCG by 5-Aza-C Treatment. If the transcriptional silencing of SNCG can be attributed to the methylation of exon 1, then demethylating the gene with 5-Aza-C should lead to expression of SNCG in both breast cancer and ovarian cancer cells. To test this, we chose two SNCG-negative breast cancer cell lines (MDA-MB435 and MCF-7), two SNCG-negative ovarian cancer cell lines (OVCAR4 and OVCAR8), and one SNCG-negative HIO cell line (HIO-135). All of these cell lines contain methylated *SNCG* gene. Cells were exposed to different concentrations of 5-Aza-C for 4–6 days, and the medium and drug were replaced daily. Fig. 10*A* shows that, in breast cancer cells, SNCG mRNA expression was induced by low doses of 5-Aza-C (0.6 μM for MCF-7 and 1 μM for MDA-MB435), and its level was increased by higher concentrations of 5-Aza-C in a dose-dependent manner. In the two ovarian tumor lines, higher doses (10 μM) of 5-Aza-C were required to induce SNCG expression as compared with 1 μM for the HIO-135 cells (Fig. 10*B*). To confirm that reactivation of SNCG expression by 5-aza-C was the result of the demethylation of the exon 1, we isolated DNA from OVCAR4 and OVCAR8, which had been treated with a 10-μM concentration of 5-aza-C, and performed bisulfite sequencing. As expected, the CpG islands in these ovarian tumor cells became unmethylated (data not shown). In contrast to SNCG-negative cell lines, 5-aza-C treatment of OVCAR3 and OVCAR5 did not further increase the level of SNCG expression. Collectively, these data clearly demonstrate that reactivation of SNCG expression by 5-Aza-C was the direct effect of demethylation of exon 1 and was not a secondary effect caused by other factors the expression of which were changed by the treatment.

DISCUSSION

The onset of cancer is associated with the silencing of the tumor suppressor genes and activation of proto-oncogenes. Previous studies have suggested that SNCG could function as an oncogene in breast cancer cells. It has been demonstrated that exogenous expression of SNCG in breast cancer cells (MDA-MB435) led to a significant

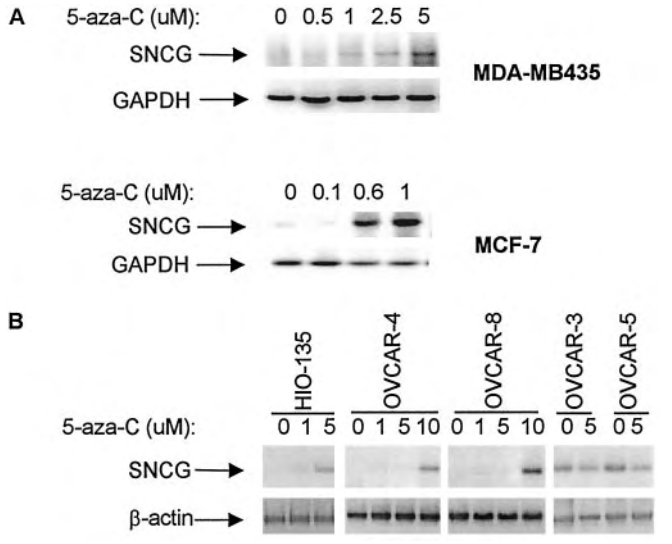

Fig. 10. Re-expression of SNCG mRNA after 5-Aza-dC treatment in breast and ovarian cancer cell lines. Breast cancer cell lines MCF-7 and MDA-MB 435 were treated with indicated doses of 5-Aza-dC for 4 days (*A*) and ovarian cancer cell lines and HIO 135 line were treated with 5-Aza-dC for 6 days (*B*). RNA from each cell line was isolated at the end of treatment, and the expressions of SNCG mRNA and GAPDH or β-actin mRNA were determined by RT-PCR.

increase in cell motility and invasiveness in cell culture and to a profound augmentation of metastasis in nude mice (24). Furthermore, exogenous expression of SNCG in MCF-7 cells significantly stimulated the growth of MCF-7 cells under anchorage-dependent (Fig. 7) and anchorage-independent conditions (33), whereas blocking SNCG expression with SNCG antisense mRNA markedly reduced the colony formation of T47D cells (25). Although previous studies by our group and others have shown that SNCG was abnormally expressed in advanced-stage breast carcinoma and ovarian carcinoma and that it is likely to be important in the pathogenesis of these neoplastic diseases, the mechanism(s) for its aberrant expression was unclear. In this report, we extensively examined the relationship between demethylation or hypomethylation of SNCG CpG island, and the expression of this candidate oncogene in breast cancer and ovarian cancer under both *in vitro* and *in vivo* conditions. From our present study, four important findings emerged.

First, in breast cancer cell lines, SNCG expression correlates with complete demethylation of the exon 1 region. By contrast, three of four SNCG-negative cell lines showed specific methylation at the CpG sites 2, 5, 7, and 10–15, suggesting that methylation at these sites is sufficient to block the expression of this gene in cell culture. More importantly, these same CpG sites were found methylated in primary breast tumor tissues and in MCF-10A, a cell line that originated from normal mammary epithelium. Thus, these data argue that, in normal mammary epithelium, SNCG is methylated at the specific CpG sites, resulting in blocking of transcription.

Semiquantitative RT-PCR, a highly sensitive detection method, failed to identify SNCG expression in six of six normal breast tissues from healthy women without cancer. This result provided new evidence to support original findings that SNCG expression was confined to malignant mammary epithelial cells. *In vivo* genomic sequencing, however, detected both methylated and unmethylated *SNCG* gene from the same normal breast tissue samples. We tentatively interpret this discrepancy thus: the unmethylated genes could be derived from other cell types such as fat cells, fibroblasts, or mononuclear leukocytes, and the lack of expression in these cells could be controlled by other mechanisms. However, our results cannot exclude the possibility that in normal mammary epithelium, SNCG is partially methylated and that partial methylation is sufficient to block its expression. Additional studies to examine SNCG expression and methylation in nonepithelial cell types of breast tissue will be needed to resolve this discrepancy. The unmethylated exon 1 in normal tissues adjacent to tumors suggests that demethylation may precede expression. A similar observation has been reported in benign and malignant colon neoplasms (9). Although the benign tumors do not express HGH, α and γ *globin* genes were hypomethylated in the promoter region of these genes just like malignant tissues, thereby suggesting that alteration in DNA methylation precedes malignancy.

The second important finding in this study is that DNA methylation also plays an important role in SNCG expression in ovarian cancer cells. Similar to breast cancer cells, an inverse relationship between exon 1 methylation and SNCG expression was found in various ovarian cancer and HIO cell lines. However, there are two characteristics that are unique and distinguish ovarian-derived epithelial cells from breast-derived epithelial cells. First, the 15 CpG sites in ovarian cancer cells were all methylated instead of being selectively methylated at the hot spots that were identified in breast cancer cells. Secondly, in ovarian cells, partial methylation permitted SNCG expression, albeit at a lower level, whereas SNCG expression could not be detected in breast cancer cells in which the exon 1 was partially and heterogeneously methylated. These differences suggest that, whereas partial methylation in the exon 1 is adequate to inhibit SNCG expression in breast cancer cells, complete methylation of the CpG island is required for silencing SNCG in ovarian cancer cells. The third finding of this study is that SNCG is expressed in three primary HMEC lines (184, 048R, and 240L) that have limited life span and that the expression correlates with hypomethylation of the exon 1. By contrast, SNCG is not expressed in normal mammary epithelial cells *in vivo* nor in the established cell line MCF-10A, and is detected at a very low level in organoids before extensive culturing. These observations suggest that SNCG expression and demethylation of the exon 1 are regulated possibly by growth factors that are present in culture medium during the establishment of HMEC cell lines. Consequently, *SNCG* gene product further stimulates cell proliferation of the primary mammary epithelial cells that normally have low growth potential. Although this is a hypothetical scenario, there is some evidence to support this hypothesis. Celis *et al.* (34) have reported that a group of genes that were not expressed in the original bladder transitional carcinomas became expressed when the tumor tissues were incubated in culture medium for a very short time (1–2 days). Synuclein was found within this group. Future studies to clearly define the function of this protein in neoplasm will provide insight to understand the molecular mechanisms that control the methylation status of *SNCG* gene.

The last important finding is that we provided direct evidence to demonstrate a stimulating role of SNCG in the growth of breast cancer cells. Transfection of SNCG into MCF-7 cells resulted in an increased proliferation rate of cells. Conversely, we also demonstrated a correlation between reduced growth rate and decreased SNCG expression. Importantly, we showed the coordinated changes in cell growth, SNCG mRNA level, and methylation status of the exon 1 of *SNCG* gene. When the HMECs, which express high levels of SNCG, are arrested by OM or by serum starvation (data not shown), the SNCG levels decrease, and the exon 1 becomes hypermethylated. At the present, the normal cellular functions of SNCG are largely unknown. Future studies to clearly define the function of this protein in neurons as well as in neoplasm will provide insight to understand the molecular mechanisms that control the methylation status of *SNCG* gene.

Currently, in the cancer research field, DNA hypermethylation has received considerable attention, and DNA hypomethylation is studied inadequately. In fact, the original observation of altered DNA methylation in cancer was hypomethylation (16). A recent study of genome-wide screening for normally methylated human CpG islands has found a considerable number of genes containing methylated CpG islands. We believe that our studies provide a clearly defined example supporting the hypothesis that abnormal hypomethylation contributes to cancer formation.

ACKNOWLEDGMENTS

We thank Dr. Martha R. Stampfer for her valuable suggestions on HMEC culturing, Dr. Zhong-Zong Pan for his helpful input, and the Tissue Bank and Biosample Repository Core Facility's (Fox Chase Cancer Center, Philadelphia, PA) staff members for providing tissue samples.

REFERENCES

1. Zheng, S., Chen, P., McMillan, A., Lafuente, A., Lafuente, M. J., Ballesta, A., Trias, M., and Wiencke, J. K. Correlations of partial and extensive methylation at the p14ARF locus with reduced mRNA expression in colorectal cancer cell lines and clinicopathological features in primary tumors. Carcinogenesis (Lond.), *21:* 2057–2064, 2000.
2. Esteller, M., Sparks, A., Toyota, M., Sanchez-Cespedes, M., Capella, G., Peinado, M., Gonzalez, S., Tarafa, G., Sidransky, D., Meltzer, S., Baylin, S., and Herman, J. Analysis of adenomatous Polyposis coli promoter hypermethylation in human cancer. Cancer Res., *60:* 4366–4371, 2000.
3. Jackson-Grusby, L., Beard, C., Possemato, R., Tudor, M., Fambrough, D., Csankovszki, G., Dausman, J., Lee, P., Wilson, C., Lander, E., and Jaenisch, R. Loss of genomic methylation causes p53-dependent apoptosis and epigenetic deregulation. Nat. Genet., *27:* 31–39, 2001.

4. Magdinier, F., and Wolffe, A. P. Selective association of the methyl-CpG binding protein MBD2 with the silent p14/p16 locus in human neoplasia. Proc. Natl. Acad. Sci. USA, *98:* 4990–4995, 2001.
5. Li, J., Cao, Y., Young, M. R., and Colburn, N. H. Induced expression of dominant-negative c-jun downregulates *NFκB* and *AP-1* target genes and suppress tumor phenotype in human keratinocytes. Mol. Carcinog., *29:* 159–169, 2000.
6. Hattori, M., and Sakamoto, H. K. T. DNA demethylase is expressed in ovarian cancers and the expression correlates with demethylation of CpG sites in the promoter region of c-*erbB-2* and *survivin* genes. Cancer Lett., *169:* 155–164, 2001.
7. Kudo, S., and Fukuda, M. Tissue-specific transcriptional regulation of *human leukosialin* (*CD43*) gene is achieved by DNA methylation. J. Biol. Chem., *270:* 13298–13302, 1995.
8. Feinberg, A. P., and Vogelstein, B. Hypomethylation distinguishes genes of some human cancers from their counterparts. Nature (Lond.), *301:* 89–91, 1983.
9. Goelz, S. E., Vogelstein, B., Hamilton, S. R., and Feinberg, A. P. Hypomethylation of DNA from benign and malignant human colon neoplasms. Science (Wash. DC), *228:* 187–190, 1985.
10. Fang, J., Zhu, S., Xiao, S., Jiang, S., Shi, Y., Chen, X., Zhou, X., and Qian, L. Studies on the hypomethylation of c-*myc*, c-*Ha-ras* oncogenes and histopathological changes in human gastric carcinoma. J. Gastroenterol. Hepatol., *11:* 1079–1082, 1996.
11. Rosty, C., Ueki, T., Argani, P., Jansen, M., Yeo, C., Cameron, J., Hruban, R., and Goggins, M. Overexpression of S100A4 in pancreatic ductal adenocarcinomas is associated with poor differentiation and DNA hypomethylation. Am. J. Pathol., *60:* 45–50, 2002.
12. Cho, M., Uemura, H., Kim, S., Kawada, Y., Yoshida, K., Hirao, Y., Konishi, N., Saga, S., and Yoshikawa, K. Hypomethylation of the MN/CA9 promoter and upregulated MN/CA9 expression in human renal cell carcinoma. Br. J. Cancer, *85:* 563–567, 2001.
13. Nakayama, M., Wada, M., Harada, T., Nagayama, J., Kusaba, H., Ohshima, K., Kozuru, M., Komatsu, H., Ueda, R., and Kuwano, M. Hypomethylation status of CpG sites at the promoter region and overexpression of the human *MDR1* gene in acute myeloid leukemias. Blood, *92:* 4296–4307, 1998.
14. Hanada, M., Delia, D., Aiello, A., Stadtmauer, E., and Reed, J. *BCL-2* gene hypomethylation and high level expression in B-cell chronic lymphocytic leukemia. Blood, *82:* 1820–1828, 1993.
15. De Smet, C., De Backer, O., Faraoni, I., Lurquin, C., Brassuer, F., and Boon, T. The activation of human gene *MAGE-1* in tumor cells is correlated with genome-wide demethylation. Proc. Natl. Acad. Sci. USA, *93:* 7149–7153, 1996.
16. Strichman-Almashanu, L. Z., Lee, R. S., Onyango, P. O., Perlman, E., Flam, F., Frieman, M. B., and Feinberg, A. P. A genome wide screen for normally methylated human CpG islands that can identify novel imprinted genes. Genome Res., *12:* 543–554, 2002.
17. Ueda, K., Fukushima, H., Masliah, E., Xia, Y., Iwai, A., Yoshimoto, M., Otero, D., Kondo, J., Ihara, Y., and Saitoh, T. Molecular cloning of cDNA encoding an unrecognized component of amyloid in Alzheimer disease. Proc. Natl. Acad. Sci. USA, *90:* 11282–11286, 1993.
18. Xia, Y., Rohan de Silva, H., Rosi, B., Yamaoka, L., Rimmler, J., Pericak-Vance, M., Roses, A., Chen, X., Masliah, E., DeTeresa, R., Iwai, A., Sundsmo, M., Thomas, R., Hofstetter, C., Gregory, E., Hansen, L., Katzman, R., Thal, L., and Saitoh, T. Genetic studies in Alzheimer's disease with a NACP/a-synuclein polymorphism. Ann. Neurol., *40:* 207–215, 1996.
19. Jakes, R., Spillantini, M., and Goedert, M. Identification of two distinct synucleins from human brain. FEBS Lett, *345:* 27–34, 1994.
20. Lavedan, C., Leroy, E., Dehejia, A., Buchholtz, S., Dutra, A., Nussbaum, R., and Polymeropoulos, M. Identification, localization and characterization of the human *ã-synuclein* gene. Hum. Genet., *103:* 106–112, 1998.
21. Ninkina, N., Alimova-Kost, M., Paterson, J., Delaney, L., Cohen, B., Imreh, S., Gnuchev, N., Davies, A., and Buchman, V. Organization, expression and polymorphism of the human *persyn* gene. Hum. Mol. Genet., *7:* 1417–1424, 1998.
22. Ji, H., Liu, Y., Jia, T., Wang, M., Liu, J., Xiao, G., Joseph, B., Rosen, C., and Shi, Y. Identification of a breast cancer-specific gene. *BCSG1*, by direct differential cDNA sequencing. Cancer Res., *57:* 759–764, 1997.
23. Bruening, W., Giasson, B., Klein-Szanto, J., Lee, V., Trojanowski, J., and Godwin, A. Synucleins are expressed in the majority of breast and ovarian carcinomas and in preneoplastic lesions of the ovary. Cancer (Phila.), *88:* 2154–2163, 2000.
24. Jia, T., Liu, Y., Liu, J., and Shi, Y. Stimulation of breast cancer invasion and metastasis by breast cancer-specific synuclein (SNCG). Cancer Res., *59:* 742–747, 1999.
25. Lu, A., Zhang, F., Gupta, A., and Liu, J. Blockade of AP1 transactivation abrogated the abnormal expression of the *breast cancer specific gene 1* in breast cancer cells. J. Biol. Chem., *277:* 31364–72, 2002.
26. Lu, A., Gupta, A., Li, C., Ahlborn, T. E., Ma, Y., Shi, E. Y., and Liu, J. Molecular mechanisms for aberrant expression of the *human breast cancer specific gene 1* in breast cancer cells: control of transcription by DNA methylation and intronic sequences. Oncogene, *20:* 5173–5185, 2001.
27. Godwin, A., Meister, A., O'Dwyer, P., Huang, C., Hamilton, T., and Anderson, M. High resistance to cisplatin in human ovarian cancer cell lines is associated with marked increase of glutathione synthesis. Proc. Natl. Acad. Sci. USA, *89:* 3070–3074, 1992.
28. Auersperg, N., Maines-Bndiera, S., Booth, J. H., Lynch, H. T., Godwin, A. K., and Hamilton, T. C. Expression of two mucin antigens in cultured human ovarian surface epithelium: influence of a family history of ovarian cancer. Am. J. Obst. Gyn., *173:* 558–565, 1995.
29. Grobelny, J., Godwin, A., and Broccoli, D. ALT-Associated PML Bodies (AA-PBs) are dynamic structures that accumulate in G_2/M phase of the cell cycle. J. Cell Sci., *113:* 4477–4485, 2000.
30. Liu, J., Li, C., Ahlborn, T. E., Spence, M. J., Meng, L., and Boxer, L. M. The expression of *p53* tumor suppressor gene in breast cancer cells is down-regulated by cytokine oncostatin M. Cell Growth Differ., *5:* 15–18, 1999.
31. Liu, J., Hadjokas, N., Mosley, B., Estrov, Z., Spence, M. J., and Vestal. R. E. Oncostatin M-specific receptor expression and function in regulating cell proliferation of normal and malignant epithelial cells. Cytokine, *10:* 295–302, 1998.
32. O'Connor, P. M., Jackman, J., Jondle, D., Bhatia, K., Magrath, D., and Kohn, K. W. Role of *p53* tumor suppressor gene in cell cycle arrest and radiosensitivity of Burkitt's lymphoma cell lines. Cancer Res., *53:* 4776–4780, 1993.
33. Liu, J., Spence, M. J., Zhang, Y. L., Jiang, Y., Liu, Y., and Shi, Y. Transcriptional suppression of synuclein γ (SNCG) expression in human breast cancer cells by the growth inhibitory cytokine oncostatin M. Breast Cancer Res. Treat., *62:* 99–107, 2000.
34. Celis, A., Rasmussen, H., Celis, P., Basse, B., Lauridsen, J., Ratz, G., Hein, B., Ostergaad, M., Wolf, H., Orntoft, T., and Celis, J. Short-term culturing of low-grade superficial bladder transitional cell carcinomas leads to changes in the expression levels of several proteins involved in key cellular activities. Electrophoresis, *20:* 355–361, 1999.

Linking Transcriptional Elongation and Messenger RNA Export to Metastatic Breast Cancers

Shanchun Guo,[1] Mohamed-Ali Hakimi,[2] David Baillat,[2] Xiaowei Chen,[1] Michele J. Farber,[1] Andres J.P. Klein-Szanto,[1] Neil S. Cooch,[2] Andrew K. Godwin,[1] and Ramin Shiekhattar[2]

[1]Department of Medical Oncology, Fox Chase Cancer Center and [2]Wistar Institute, Philadelphia, Pennsylvania

Abstract

The biochemical pathways that are disrupted in the genesis of sporadic breast cancers remain unclear. Moreover, the present prognosticating markers used to determine the prognosis of node-negative patient leads to probabilistic results, and the eventual clinical course is far from certain. Here we identified the human TREX complex, a multiprotein complex that links transcription elongation to mRNA transport, as culprit of aggressive human breast cancers. We show that whereas p84N5 (called hTREX84) is expressed at very low levels in normal breast epithelial cells, it is highly expressed in breast tumors. Importantly, hTREX84 expression correlates with tumor size and the metastatic state of the tumor progression. Reduction of hTREX84 levels in breast cancer cell lines by small interfering RNA result in inhibition of cellular proliferation and abrogation of mRNA export. These results not only identify hTREX84 as a prognosticator of breast cancer but also delineate human TREX complex as a target for therapeutic drugs against breast cancer. (Cancer Res 2005; 65(8): 3011-6)

Introduction

Metastatic tumors are the most prevalent cause of death in cancer patients. A major aim in studying metastasis is to understand the mechanism by which cancer cells acquire distinct genetic and epigenetic changes that result in their progression through metastatic states. Recent experiments using microarray studies have expanded our understanding of metastasis in various human tumor samples (1, 2). Although such studies have been powerful for producing gene expression fingerprints of metastatic tumor cells, it has been difficult to assess the contribution of individual genes to the metastasis progression. Breast cancer is the most common malignancy in women and it could be effectively cured if diagnosed at an early stage. The most commonly used predictive molecular markers for breast cancer include Ki-67, estrogen receptor (ER), progesterone receptor (PR), and human epidermal growth factor receptor 2 (HER2) (3). We searched for new prognostic markers that not only could be predictive of the more aggressive forms of breast cancers but also could further provide mechanistic insight into the molecular mechanism underlying metastasis. In this study, we describe the increased expression of TREX84, a subunit of a multiprotein complex involved in transcriptional elongation and mRNA export, in human breast cancer and its intimate association with breast cancer progression and metastasis.

Note: S. Guo and M-A. Hakimi contributed equally to this work.

Requests for reprints: Ramin Shiekhattar, Wistar Institute, 3601 Spruce Street, Philadelphia, PA 19104. Phone: 215-898-3896; Fax: 215-898-3986; E-mail: Shiekhattar@wistar.upenn.edu.

Materials and Methods

Primary breast cancer specimens. Human breast tissue specimens used in this study were collected following NIH guidelines and using protocols approved by the Institutional Review Board at Fox Chase Cancer Center. These specimens were surgically obtained from breast cancer patients at Fox Chase from 1991 to 2002. A total 72 primary breast cancer were examined which included 69 invasive ductal carcinomas and 3 invasive lobular carcinomas. Seventy females and two males were included in the study. Ninety percent (65 of 72) of the patients were Caucasian (i.e., white non-Hispanic), 8% (6 of 72) were African American, and 1% (1 of 72) were Asian. The age range was 31 to 97 years with a median age of 56 years. Grading of histologic malignancy of each specimen was assessed according to the system as reported previously (4, 5). Lymphonodal metastatic status was determined by histopathologic examination in each case according to the pTNM classification as proposed by the American Joint Committee on Cancer. Thirty-seven paired normal breast tissues were also obtained from the above patients. All of the samples were snap frozen in liquid nitrogen and kept at −80°C until used. Tissue extracts were prepared as previously described (6).

Affinity purification of Flag-p84. Flag-p84 and a selectable marker for puromycin resistance were cotransfected into HeLa cells. Transfected cells were grown in the presence of 5 mg/mL puromycin, and individual colonies were isolated and analyzed for Flag-p84 expression. To purify the p84 complex, nuclear extract from the Flag-p84 cell line was incubated with anti-Flag M2 affinity gel (Sigma, St. Louis, MO), and after extensive washing with buffer A [20 mmol/L Tris-HCl (pH 7.9), 0.5 mol/L KCl, 10% glycerol, 1 mmol/L EDTA, 2 mmol/L $MgCl_2$, 5 mmol/L DTT, and 0.5% NP40], the affinity column was eluted with buffer A containing Flag peptide (500 mg/mL) according to manufacturer's instructions (Sigma). p84-containing eluate were fractionated on a Superdex 200 (Pharmacia, Peapack, NJ) equilibrated in 0.5 mol/L KCl in buffer A containing 0.1% NP40 and 1 μg/mL aprotinin, leupeptin, and pepstatin. Analysis of nuclear extract on Superose 6 was as described previously (7).

Glutathione *S*-transferase pulldown with UAP56. Control glutathione *S*-transferase (GST, lanes 1) or GST-UAP56 (lane 2) was incubated with HeLa nuclear extract. After washing with BC500 buffer [20 mmol/L Tris-HCl (pH 8), 500 mmol/L KCl, 10% glycerol, 0.2 mmol/L EDTA, and 1 mmol/L phenylmethylsulfonyl fluoride] proteins bound to GST-UAP56 or GST were analyzed by Western blot with p84 antibodies.

Organoid isolation, cell lines, and cell culture. Media and cell culture reagents were prepared by the Cell Culture Facility at Fox Chase Cancer Center. Eighteen cases of organoids were separated and prepared by using collagenase digestion as described previously (8, 9). Six primary cultures of human breast epithelial cells were established and cultured in 199 Medium with 15% fetal bovine serum and insulin (290 units per 500 mL). Six primary cultures of human breast fibroblast cells were cultured in DMEM supplemented with 20% FBS and 1× antibiotic-antimycotic solution. Human breast cancer cell lines MDA-MB-231, MDA-MB-435, MDA-MB-468, MCF-7, BT-20, and ZR-75-1 were cultured in DMEM supplemented with 10% FBS and 1× antibiotic-antimycotic solution. T47D cells were maintained in RPMI supplemented with 10% FBS and 0.2 unit/mL of pork insulin. SKBP-3 cells were maintained in McCoy's 5a medium supplemented with 15% FBS.

Immunofluorescence. Cells grown in monolayer cultures were fixed with 4% paraformaldehyde in PBS, permeabilized with 0.2% Triton X-100,

and blocked with 10% FCS before antibody staining. Staining by anti-p84 antibodies was visualized with corresponding fluorescein-labeled secondary antibody. All images were acquired with a bio-Rad MRC1000 confocal microscope.

Western blotting assay. After cell lysates were obtained from cell lines or tissues, 30 μg of total protein from each sample were analyzed by Western blotting. Protein extracts were electrophoresed on a 4% to 20% Tris-glycine gel, and the separated proteins were electrophoretically transferred to nitrocellulose for immunodetection. The membrane was blocked in 5% nonfat dry milk in TBST for 1 hour at room temperature and incubated with monoclonal antibody to human p84N5 at a dilution of 1:2000 in TBST + 2.5% nonfat dry milk, followed by horseradish peroxidase-conjugated antimouse secondary antibody (Amersham, Piscataway, NJ) at a dilution of 1:10,000. Immunoblots were reprobed with β-actin monoclonal antibody to confirm equal loading. MDA-MB-435 cell extracts were used as a control sample in each of the experiments. The expression levels of p84 and β-actin detected by immunoblotting were quantitated using the program IMAGE (NIH) for the integrated density of each band. Western blot assays were conducted in duplicate for each sample and the mean value was used for the calculation of protein expression levels.

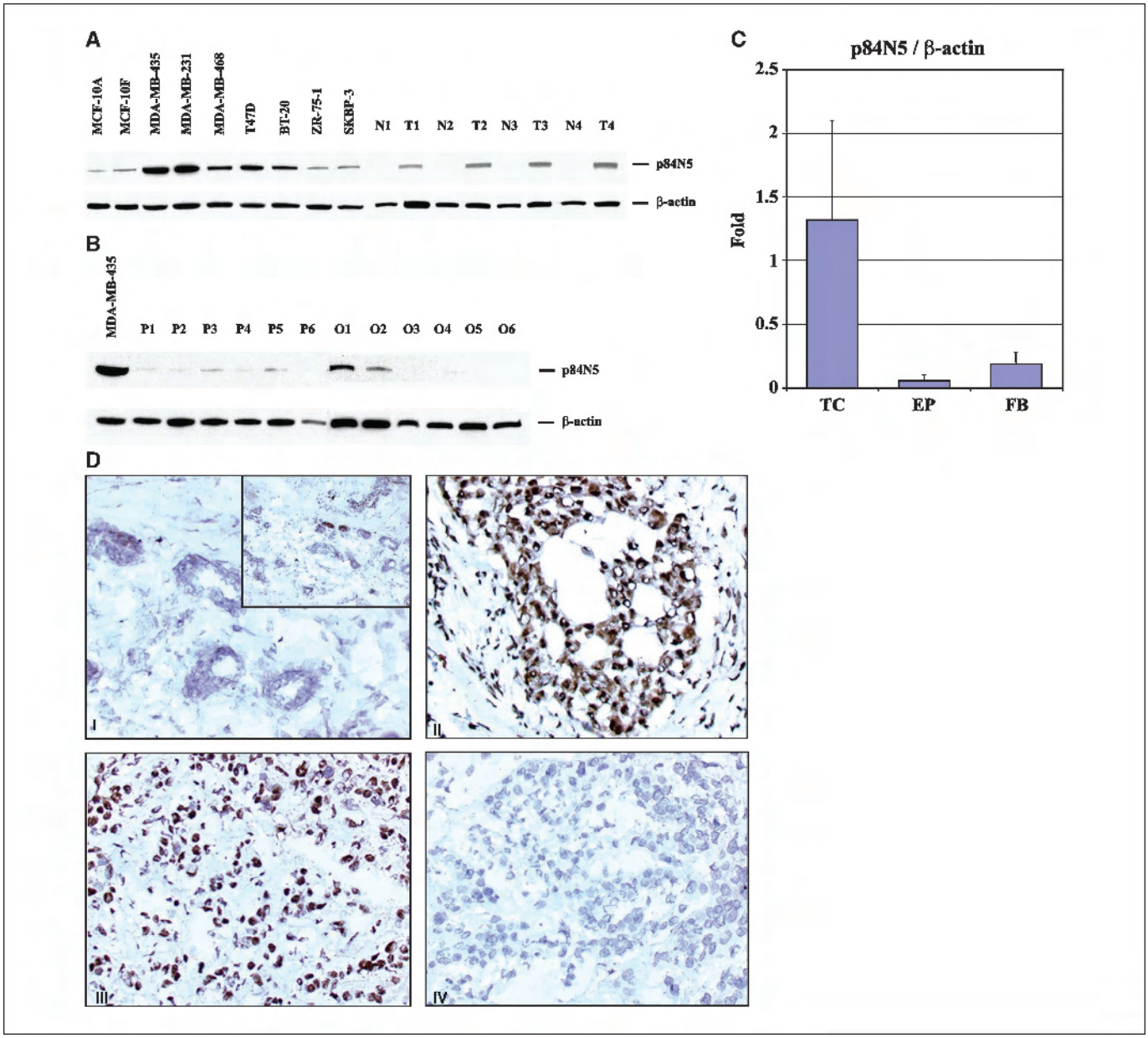

Figure 1. p84N5 is aberrantly expressed in breast cancer. *A,* p84N5 protein expression in immortal breast epithelial cell lines (MCF-10A and MCF-10F), breast tumor cell lines, paired normal (N1-4), and breast cancer (T1-4) tissues. Protein samples were separated on a SDS-polyacrylamide gel and proteins were immunoblotted using anti-p84N5 or β-actin monoclonal antibodies. *B,* p84N5 protein expression in primary breast epithelial cell cultures (P1-P6) and purified organoids (O1-O6) by Western blotting. *C,* p84N5/β-actin ratio in breast cancer cell lines (*TC*), primary breast epithelial cell cultures (*EP*), fibroblast cell cultures (*FB*). *D,* immunohistochemical analysis of frozen sections of normal breast tissue and breast tumor specimens for the p84N5 protein. *I,* p84N5 is weakly expressed in the cytoplasm and nuclei of normal ductal epithelia and lobular epithelia. A few epithelial structures showed moderate immunostain. *Inset,* same region at lower magnification to show overall staining pattern with only few moderately stained ductal structures. *II,* p84N5 is intensively expressed in the cytoplasm and nuclei of a grade 1 invasive ductal carcinoma. *III,* p84N5 is expressed at high levels exclusively in the nuclei of a grade 3 invasive ductal carcinoma. *IV,* previous tumor section evaluated without the primary antibody to serve as a negative control. Magnification 200×.

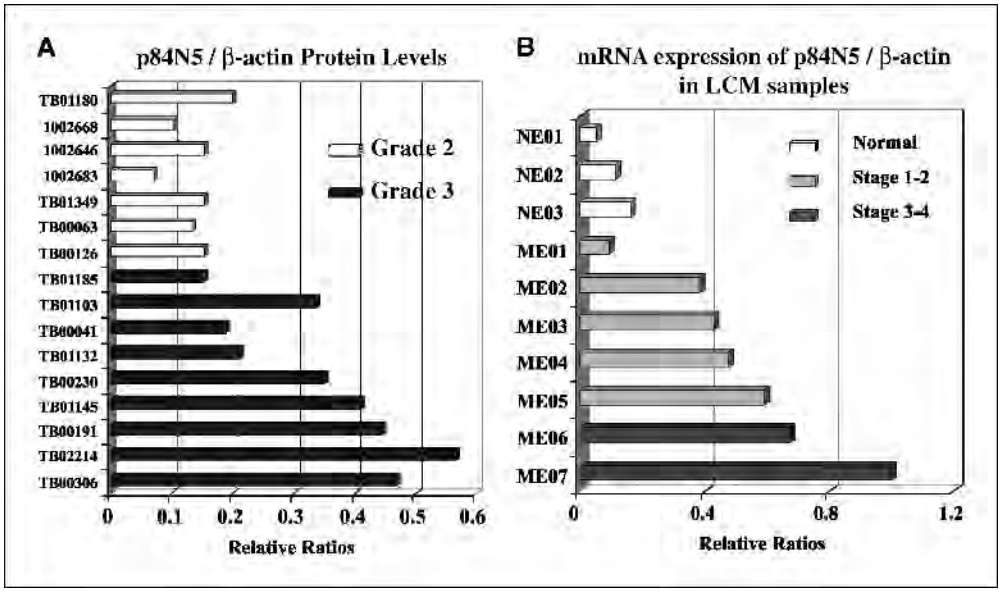

Figure 2. p84N5 displays increased expression in late-stage tumors. *A,* expression of p84N5 by Western blot analysis in the same grade 2 and 3 breast tumors as evaluated. *B,* quantitative real-time PCR analysis of normal mammary lobular epithelial cells (*NE*) and malignant epithelial (*ME*) cells captured by laser capture microdissection. All tumors were grade 3 and were separated based on clinical staging [i.e., combined primary tumor staging (*Tis*), nodal staging (*N0*), and metastatic staging (*M0*)]. ME01-05 were determined to be stage I and II breast tumors, whereas ME06-07 were stage III and IV tumors according to the *AJCC Staging Manual*.

Immunohistochemistry. p84N5 protein immunostaining was carried out with mouse monoclonal p84N5 antibody (Novus Biologicals, Littleton, CO), at a dilution of 1:100. Because the antibody available does not recognize p84N5 in formalin-fixed, frozen sections were used. For frozen section immunohistochemistry, the sections were fixed in cold acetone for 10 minutes and rinsed in cold PBS for 5 minutes. The sections were then incubated in methanol/0.3% hydrogen peroxide for 10 minutes, washed with PBS, and treated with 0.1% Triton X-100 in PBS for 5 minutes and washed with PBS again. The sections were then incubated at 4°C overnight with p84N5 antibody. Reaction products were visualized by immersing the glass slides in 3,3-diaminobenzidine tablet sets (Sigma Fast, Sigma) and counterstained with hematoxylin. A positive control was included in each experiment. As negative controls, either the p84N5 antibody was omitted or sections were washed in 1× PBS.

Laser capture microdissection. Laser capture microdissection (LCM) was done as previously described with minor modification (7). In brief, frozen normal and tumor breast tissue samples were embedded in ornithine carbamyl transferase medium, sectioned in a cryostat at 8-μm thickness, and mounted on nonadhesive glass slides. Fixation was done in 70% ethanol for 60 seconds. Breast epithelial cells were visualized by H&E staining. H&E-stained frozen sections were dehydrated for 30 seconds in 70%, 95%, and 100% ethanol with a final 2-minute dehydration step in xylene. Air-dried sections were then laser captured and microdissected by a PixCell II LCM system (Arcturus Engineering, Mountain View, CA). The normal or malignant mammary epithelial cells to be selectively microdissected away from stroma were identified and targeted through a microscope, and a 15-μm laser beam pulse activated the film on a CapSure LCM Cap (Arcturus Engineering). Approximately 5×10^3 cells were captured for each specimen. Based on careful review of the histologic sections, each microdissection is estimated to contain ~90% of the desired cells. After microdissection, 100 μL of guanidinium isothiocyanate-containing lysis buffer with 0.7 μL mercaptoethanol were applied directly to the microdissected cells adhered on the CapSure LCM cap, samples were placed into a 0.5-mL microfuge tube, and vortexed vigorously. Total RNAs were extracted using the Strata Prep Total RNA Microprep Kit (Stratagene, La Jolla, CA). A DNase treatment was done according to the manufacturer's recommendations. The RNA was resuspended in 20 μL of RNA elution buffer. After being reconcentrated by vacuum without heat, total RNA from each LCM sample was reverse transcribed in a 20-μL reaction as described above.

Quantitative real-time PCR analysis. cDNA mixture (0.63 μL) above was used in a real-time PCR reaction (25 μL total volume) done with Smart Cycle TD (Cepheid, Sunnyvale, CA) following methods recommended by the manufacturer. Optimal conditions were defined as step 1, 95°C for 10 minutes; step 2, 95°C for 15 seconds and 60°C for 60 seconds with Optics, repeated for 50 cycles. The relative mRNA expressions of *p84N5* were adjusted with *ACTB*. The primer and probe sets used for real-time PCR were as follows: *p84N5*, forward primer 5′-GGAACCCTGTGCAATGCTATG-3′ and reverse primer 5′-ACATGTTCTCCTCCTGTTTTCAATT-3′; Taqman probe, (FAM) 5′-ATAAATTAGATGATACTCAGGCCTCAAGAAAAAAGATGGA-3′ (BHQ1). *ACTB*: forward primer 5′-GCCAGGTCATCACCATTGG-3′ and reverse primer 5′-GCGTACAGGTCTTTGCGGAT-3′; Taqman probe, (Cal red) 5′-CGGTTCCGCTGC CCTGAGGC-3′ (BHQ2).

Small interfering RNA transfection and cell proliferation. The small interfering RNA (siRNA) sequences targeting *p84N5* corresponded to the coding region 1652 to 1672 (5′-AATGATGCTCTACTGAAGGAA-3′) relative to

Table 1. Relationship between p84 protein expression and clinicopathologic variables

	n	Mean	Lower bound	Upper bound	*P*
Menopausal status					
Premenopausal	27	0.280	0.165	0.396	0.375
Postmenopausal	45	0.180	0.139	0.260	
Tumor size (cm)					
≤2	21	0.134	0.078	0.191	0.015
>2	50	0.285	0.234	0.363	
Lymph node metastasis					
Negative	31	0.131	0.077	0.185	0.002
Positive	36	0.329	0.232	0.425	
Histologic grade					
2	18	0.143	0.053	0.233	0.033
3	51	0.283	0.213	0.354	
Estrogen receptor					
Negative	23	0.32	0.193	0.448	0.063
Positive	36	0.177	0.122	0.247	
Progesterone receptor					
Negative	28	0.331	0.219	0.442	0.011
Positive	31	0.147	0.092	0.219	

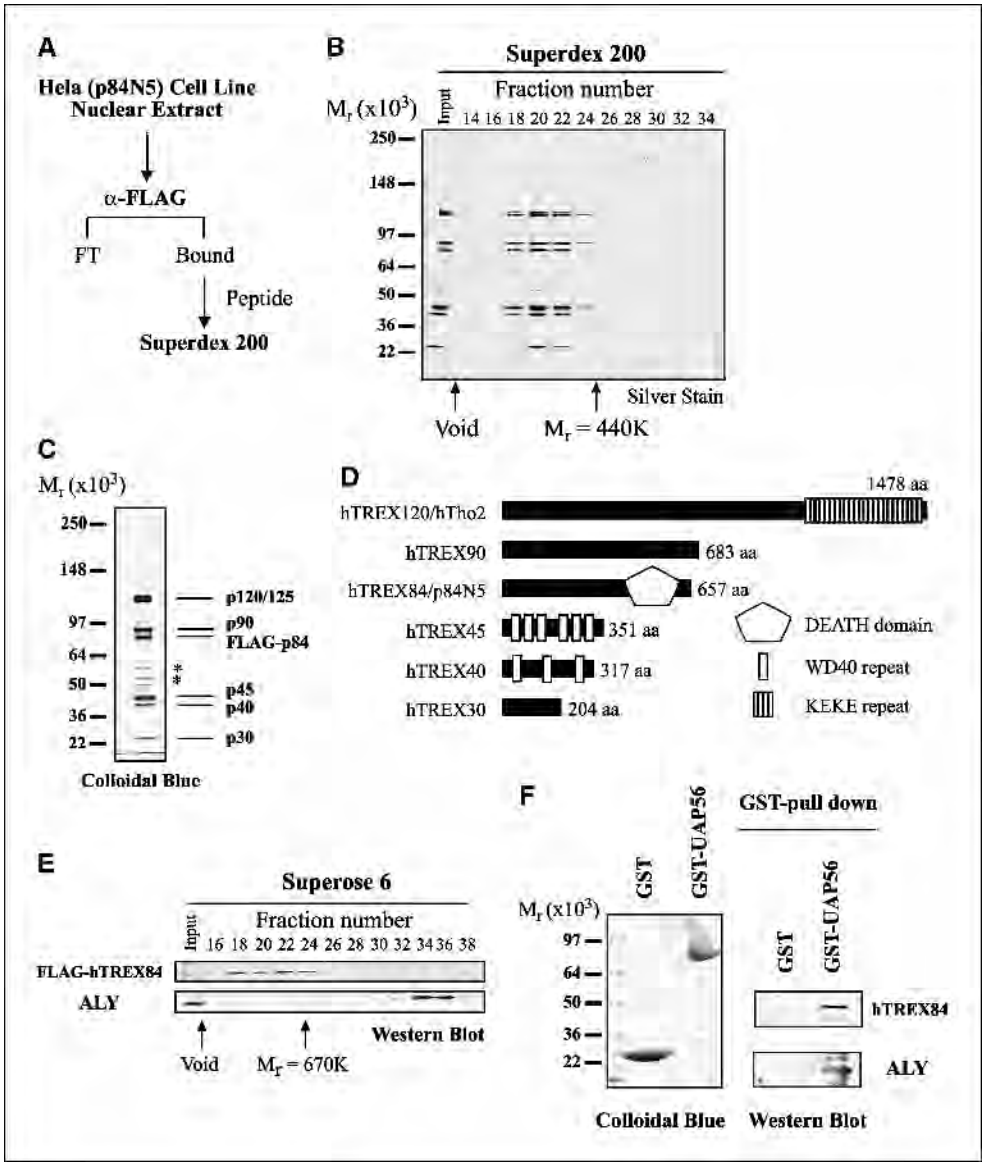

Figure 3. p84N5 is a component of the human TREX complex. *A,* schematic of p84N5 isolation using a 293-derived Flag-tagged cell line. *B,* human TREX complex isolated using the protocol shown in (*A*) was analyzed by silver staining following fractionation on the Superset 200. *C,* colloidal blue analysis of Flag-affinity eluate shown in (*A*). Individual bands were excised and subjected to mass spectrometric sequence analysis. *D,* diagrammatic representation of human TREX subunits. hTREX120, hTREX90, hTREX45, hTREX40, and hTREX30 correspond to Genbank accession nos. AL030996, XM_037945, NM_032361, NM_024339, and BC020599, respectively. *E,* analysis of nuclear extract using Superose 6 gel filtration. Column fractions were analyzed by Western blotting using antibodies (*right*). *D,* GST or GST-UAP56 were used for affinity-purification of human REX and ALY proteins.

the start codon. The corresponding siRNA duplexes with the following sense and antisense sequences were used: 5′-UGAUGCUCUACUGAAGGAAdTdT (sense) and dTdTACUACGAGAUGACUUCCUU-5′ (antisense). A nonspecific control XI siRNA duplex had the following sequences: 5′-AUAGAUAAG-CAAGCCUUACUU (sense) and UUUAUCUAUUCGUUCGGAAUGP-5′ (antisense). All of the siRNA duplexes were synthesized by Dharmacon Research, Inc. (Lafayette, CO) using 2′-ACE protection chemistry.

Cells in the exponential phase of growth were plated at 30% confluence in 6-cm plates, grown for 24 hours, and transfected with siRNA (p84N5 siRNA: 200 nmol/L) using oligofectamine and OPTI-MEM I reduced serum medium (Invitrogen Life Technologies, Inc., Carlsbad, CA), according to the manufacturer's protocol. The concentrations of siRNAs were chosen based on dose-response studies. Silencing was examined 24, 48, and 72 hours after transfection. Control cells were treated with oligofectamine (mock) or transfected using a control siRNA. Cell proliferation and apoptosis was examined using Guava ViaCount and Nexin assays, respectively as previously described (10). All studies were done in triplicates.

Statistical methods. Statistical analyses, including χ^2 and t test, were done using Microsoft Excel software. All statistical tests were two sided, and Ps < 0.05 were considered to be statistically significant. Error bars represent 95% confidence intervals.

Results and Discussion

To identify novel genes whose aberrant regulation may result in sporadic breast cancer, we analyzed the expression profiles of genes in breast tumors using public databases. We focused on p84N5, a nuclear protein containing a DEATH-domain previously reported to associate with *Rb* (11, 12), as one of the genes that displayed increased expression in breast cancers. To directly analyze the expression of p84N5 in breast cancers, we compared the p84N5 protein levels in the breast cancer tissues and the surrounding normal tissues using Western blot analysis. As Fig. 1*A* indicates, whereas cancerous tissues displayed high levels of p84N5 expression, the levels of p84N5 in normal tissues were nearly undetectable (compare N1 through N4 and T1 through T4). Similar increased expression of p84N5 is evident comparing breast cancer cell lines and normal primary epithelial cells or breast organoids (Fig. 1*A* and *B*). We substantiated these results by examining the expression of p84N5 using real-time PCR and immunohistochemistry. Using frozen sections, we detected by immunohistochemistry that normal breast tissue displayed a heterogeneous expression

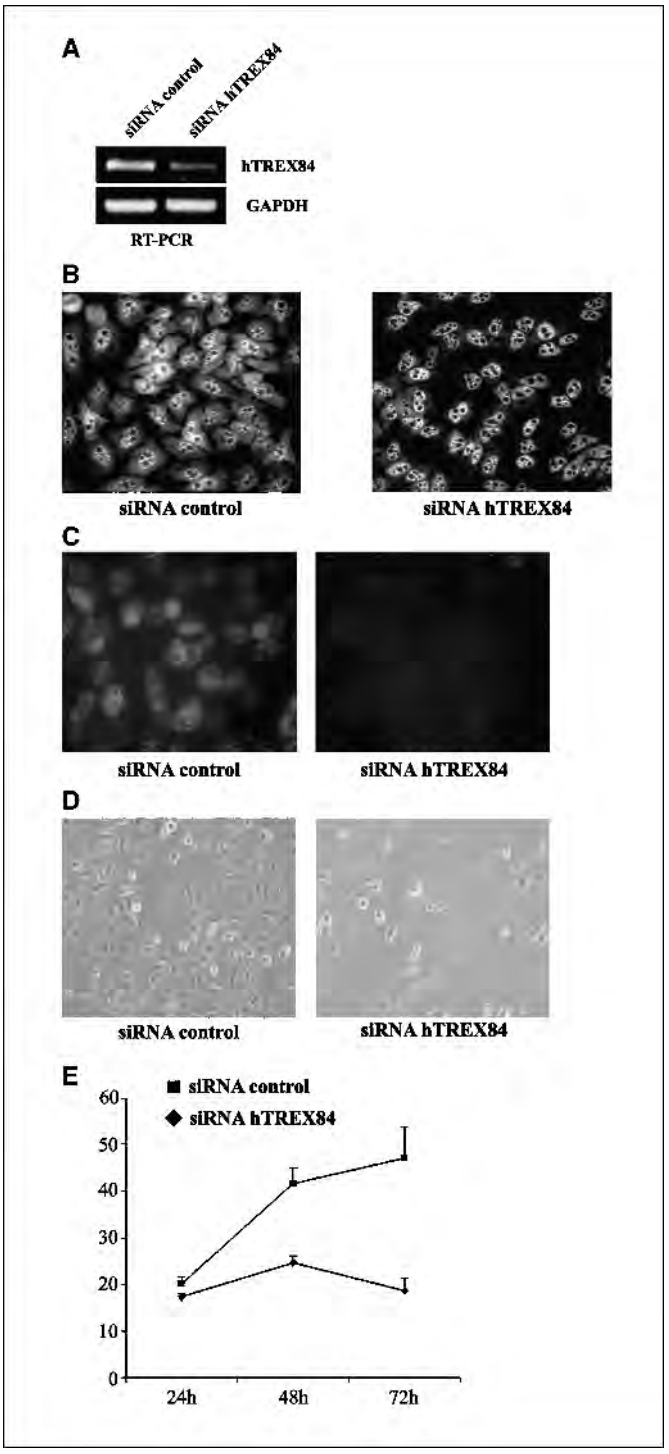

Figure 4. Knock down of TREX84 leads to defects in mRNA export and cellular proliferation. *A,* analysis of TREX84 and GAPDH mRNA levels following treatment of HeLa cells with siRNA against TREX84 or control siRNA. *B,* treatment of HeLa cells with siRNA against TREX84 or control siRNA; treatment of cells with siRNA against TREX84 results in accumulation of mRNA in the nucleus. *C,* analysis of TREX84 expression following siRNA treatment for 72 hours by immunofluoresence staining in MDA-MB-231 tumor cells (*left,* cells transfected with control siRNA; *right,* cells treated with TREX84-siRNA). *D,* photomicrographs show the morphology of the MDA-MB-231 cells following abrogation of TREX84 expression (*left,* tumor cells transfected with control siRNA; *right,* cells treated with TREX84-siRNA). *E,* cell proliferation of breast tumor cells following abrogation of TREX84. Cell proliferation and apoptosis (data not shown) was examined using Guava ViaCount and Nexin assays, respectively. Plotted is the number of viable cells ($\times 10^4$) at 24, 48, and 72 hrs after treatment with control siRNA or with TREX84-siRNA. Three independent experiments.

pattern with a few ductal and lobular epithelial structures exhibiting moderate expression of p84N5, whereas most of the normal breast showed mild or negative expression of the protein (Fig. 1*D*, *I*). Conversely, ductal carcinomas showed an intense and homogeneous expression of p84N5, which is consistent with the Western blot analysis (Fig. 1*C* and *D*, *II-IV*).

We next asked whether p84N5 expression levels were indicative of the aggressive nature of the breast cancers. Comparison of early-stage tumors (grade 2) and those of later stages (grade 3) revealed a marked elevation of p84N5 RNA and protein levels in late-stage tumors (Fig. 2*A* and data not shown). Importantly, analysis of p84N5 levels in a large number of tumors revealed a strong relationship between p84N5 expression levels and lymph node metastasis ($P = 0.002$) and tumor size ($P = 0.015$; Table 1). Other prognostic indicators, including ER positivity ($P = 0.063$) and histologic grade ($P = 0.033$) were also found to be associated with increased p84N5 protein levels. To further confirm these results, lobular epithelial cells from normal breast tissues and malignant epithelial cells from grade 3 tumors were captured by laser capture microdissection and p84N5 levels were analyzed by quantitative real-time PCR (Fig. 2*B*). As Fig. 2*B* attests, the expression levels of p84N5 transcripts are elevated in all but one of the tumors as compared with histologically normal epithelial cells. When these tumors were subdivided based on clinical staging [combined T (tumor size), N (nodal involvement), M (metastatic) classification], p84N5 levels correlated with more aggressive tumors (stage I-II versus III-IV). Taken together, these data indicate that p84N5 is highly expressed in breast cancers and its expression is strongly associated with an aggressive phenotype of human breast tumors.

To gain insight into the biological role of p84N5, we isolated a p84N5-containing multiprotein complex from mammalian cells. This was accomplished by developing a 293-derived stable cell line expressing Flag-tagged p84N5. Figure 3*A* depicts the purification of Flag-p84N5 using anti-Flag antibodies followed by the analysis of the Flag-p84N5 eluate using gel filtration chromatography. This analysis revealed the specific association of p84N5 with polypeptides of 125, 120, 90, 45, 40, and 30K (Fig. 3*B* and *C*). Interestingly, mass spectrometric sequencing of p84N5-associated polypeptides revealed the identity of p84N5 associated proteins as the human counter parts of the yeast TREX complex reported to couple transcriptional elongation and mRNA export (Fig. 3*D*; refs. 13, 14). Therefore, we have termed this complex human TREX and p84N5 as hTREX84. Importantly, in contrast to the yeast TREX complex, the human complex was devoid of the RNA export and splicing factors ALY and UAP56 (13). We therefore asked whether endogenous ALY and hTREX84 form a stable complex which is reflected by coelution of the two proteins on gel filtration. Analysis of HeLa nuclear extract by Superose 6 sizing fractionation showed distinct chromatographic elution profiles for hTREX84 and ALY proteins indicating that the two proteins are not stably associated (Fig. 3*E*). However, consistent with a previous report (13), we observed the association of hTREX and ALY through the UAP56 protein (Fig. 3*F*), and that hTREX and ALY colocalize in breast tumor cells as determined by immunofluorescence assays (data not shown). These results indicate that whereas hTREX and ALY may not be stably associated, their interaction is promoted by the UAP56 protein.

The yeast TREX complex was shown to be intimately involved in the export of mRNA to the cytoplasm (13, 14). We therefore, asked whether human TREX also plays a role in mRNA export.

mRNA was visualized using immunofluorescent analysis using oligo-dt as probes. To address the role of human TREX in mRNA export, hTREX84 protein was depleted using siRNA against hTREX84 following which mRNA levels were analyzed (Fig. 4*A*). Whereas the mRNA in cells treated with control siRNA could be visualized in both the cytoplasmic and the nuclear domains, treatment of cells with siRNA against hTREX84 resulted in the accumulation of mRNA in the nucleus and the loss of cytoplasmic mRNA (Fig. 4*B*). These results indicate that similar to the role for yeast TREX complex, hTREX plays a pivotal function in mRNA export.

Because hTREX84 is highly expressed in aggressive forms of breast cancer, we asked whether reduction of hTREX84 concentrations may slow the proliferative capacity of breast cancer cells. Human breast cancer cell lines express high levels of hTREX84 compared with that of primary breast epithelial cells and organoids (Fig. 1*A* and *B*). To address the proliferative potential of hTREX84, we treated MDA-MB-231 breast cancer cell line with siRNA against hTREX84 (Fig. 4*C*). Treatment of breast cancer cells with siRNA against hTREX84 potently and specifically reduced the proliferative potential of these cells (Fig. 4*D* and *E*). Analyses of these cells using a GuavaNexin assay found no statistically difference for Annexin V-PE and 7-AAD positive cells in siRNA treated cells, indicating the absence of induction of apoptosis (data not shown). Taken together, our finding suggest a role for the hTREX complex in cellular proliferation and following confirmation by other studies conducted among different populations in the future, hTREX84 may serve as a prognostic marker for aggressive forms of human breast cancer. Furthermore, therapeutic interventions that target human TREX should be of tremendous value in the fight against breast cancer.

Acknowledgments

Received 10/11/2004; revised 11/29/2004; accepted 2/8/2005.

Grant support: Eileen Stein-Jacoby Fund fellowship (X. Chen), Department of Defense Breast Cancer Research Program W81XWH-04-1-0573, Department of Defense Breast Cancer Research Program (U.S. Army Medical Research) grant DAMD17-03-1-0312 (A.K. Godwin), NIH Ovarian Cancer Specialized Programs of Research Excellence grant P50 CA83638, Commonwealth of Pennsylvania appropriation, NIH grant CA90758-03 (R. Shiekhattar), and U.S. Army Medical Research grant DAMD17-02-1-0632 (R. Shiekhattar).

The costs of publication of this article were defrayed in part by the payment of page charges. This article must therefore be hereby marked *advertisement* in accordance with 18 U.S.C. Section 1734 solely to indicate this fact.

We thank the support of the Tumor Bank, Biosample Repository, Cell Imaging, DNA Sequencing, Flow Cytometry and Cell Sorting, and Histopathology Core Facilities at Fox Chase and Michael Green for providing ALY antibody and the plasmid encoding UAP56.

References

1. Ramaswamy S, Ross KN, Lander ES, Golub TR. A molecular signature of metastasis in primary solid tumors. Nat Gene 2003;33:49–54.
2. van't Verr LJ, Dai H, van de Vijver MJ, et al. Gene expression profiling predicts clinical outcome of breast cancer. Nature 2002;415:530–6.
3. Esteva FJ, Hortobagyi GN. Prognostic molecular markers in early breast cancer. Breast Cancer Res 2004;6:109–18.
4. Bloom HJG, Richardson WW. Histological grading and prognosis in cancer. A study of 1409 cases of which 359 have been followed for 15 years. Br J Cancer 1957;11:359–77.
5. Elston CW, Ellis IO. Pathological prognostic factors in breast cancer. I. The value of histological grade in breast cancer: experience from a large study with long term follow-up. Histopathology 1991;19:403–10.
6. Bruening W, Giasson BI, Klein-Szanto AJ, Lee VM, Trojanowski JQ, Godwin AK. Synucleins are expressed in the majority of breast and ovarian carcinomas and in preneoplastic lesions of the ovary. Cancer 2000; 88:2154–63.
7. Dong Y, Hakimi MA, Chen X, et al. Regulation of BRCC, a holoenzyme complex containing BRCA1 and BRCA2, by a signalosome-like subunit and its role in DNA repair. Mol Cell 2003:12:1087–99.
8. Russo J, Calaf G, Russo IH. A critical approach to the malignant transformation of human breast epithelial cells. Crit Rev Oncog 1993;4:403–7.
9. Russo J, Russo IH. Development of the human breast. In: Encyclopedia of reproduction. Knobil E and Neill JD, editors. New York: Academic Press; 1998: 3:71–80.
10. Frolov A, Chahwan S, Ochs M, et al. Response markers and the molecular mechanisms of action of Gleevec in gastrointestinal stromal tumors. Mol Cancer Ther 2003;2:699–709.
11. Durfee T, Mancini MA, Jones D, Elledge SJ, Lee WH. The amino-terminal region of the retinoblastoma gene product binds a novel nuclear matrix protein that co-localizes to centers for RNA processing. J Cell Biol 1994;127:609–22.
12. Doostzadeh-Cizeron J, Evans R, Yin S, Goodrich DW. Apoptosis induced by the nuclear death domain protein p84N5 is inhibited by association with Rb protein. Mol Biol Cell 1999;10:3251–61.
13. Strasser K, et al. TREX is a conserved complex coupling transcription with messenger RNA export. Nature 2002;417:304–8.
14. Jimeno S, Rondon AG, Luna R, Aguilera A. The yeast THO complex and mRNA export factors link RNA metabolism with transcription and genome instability. EMBO J 2002;21:3526–35.

Involvement of RHO GTPases and ERK in synuclein-γ enhanced cancer cell motility

ZHONG-ZONG PAN[1,2], WENDY BRUENING[2,3] and ANDREW K. GODWIN[2]

[1]Department of Animal Science, University of Vermont, 570 Main Street, Burlington, VT 05405;
[2]Department of Medical Oncology, Fox Chase Cancer Center, 333 Cottman Avenue, Philadelphia, PA 19111, USA

Received May 8, 2006; Accepted July 7, 2006

Abstract. Synuclein-γ is aberrantly expressed in more than 70% of stage III/IV breast and ovarian carcinomas. Ectopic overexpression of synuclein-γ enhanced MDA-MB-435 cell migration *in vitro* and metastasis in a nude mouse model. However, the mechanism of how synuclein-γ promotes cell motility is not clear. In our previous studies, we showed that synuclein-γ overexpression activates ERK. In the present study, we overexpressed synuclein-γ in several breast and ovarian cancer cell lines and evaluated the effect of synuclein-γ on the activity of small G-protein RHO family members. We found that at least one of the RHO/RAC/CDC42 GTPases showed a higher level of the GTP-bound active form. Consistent with their role in regulating the intracellular motile machinery, inhibition of the RHO/RAC/CDC42 by *C. difficile* Toxin B blocked cell migration in both parental cells and synuclein-γ overexpressing cells. The ERK inhibitor U0126 also blocked the cell migration in both parental cells and synuclein-γ overexpressing cells. Collectively, our data indicate that synuclein-γ might be involved in late stage breast and ovarian cancer metastasis by enhancing cell motility through activation of the RHO family small-GTPases and ERK.

Introduction

The synucleins (synucleins-α, -ß, -γ, and synoretin) are a family of small, highly soluble proteins that are normally expressed predominantly in neurons (1,2). Although the expression patterns and abundance of the synucleins suggest their importance in neuron development and function, very little is known about their physiological functions. Among the synuclein proteins, synuclein-α is associated with neurodegenerative diseases such as Parkinson's disease and Alzheimer's disease (1,3). Synuclein-γ, also referred to as breast cancer specific gene 1 (BCSG1), has been identified to be aberrantly up-regulated in breast and ovarian cancers (4,5). Abnormal expression of synuclein-γ has also been identified in several other cancer types including bladder and colorectal carcinomas, glaucoma, and brain tumor (6-10). The abnormal expression of synuclein-γ in cancer cells is caused by the loss of epigenetic control as a result of hypomethylation of the CpG island in the synuclein-γ gene (11).

The expression of synuclein-γ in primary breast and ovarian cancers is strongly associated with advanced stages of tumor progression. Synuclein-γ is not expressed in normal or benign breast and ovarian tissues, but is highly expressed in the vast majority (>70%) of stage III/IV breast and ovarian tumors (4,5). Several lines of evidence suggest that synuclein-γ might be a malignant factor. In our previous studies, we found that synuclein-γ can promote cell survival and inhibit stress- and microtubule inhibitory drug-induced apoptosis by modulating JNK and ERK pathways (12). In breast cancer cells, synuclein-γ can activate estrogen receptor (ER), promote cell proliferation, and inhibit mitotic checkpoint control (13-18). In breast cancer cell line MDA-MB-435 cells, ectopic overexpression of synuclein-γ enhanced cell migration *in vitro* as well as metastasis in a nude mouse model (19). The mechanism of how synuclein-γ promotes cell motility is not clear. Up-regulation of matrix metalloproteinases-2 and -9 (MMPs) by synuclein-γ has been found in retinoblastoma Y79 cells, but MMP-2 and MMP-9 were not found activated in MDA-435 cells that overexpress synuclein-γ (19,20).

Cell migration and invasion involves dynamic changes in extracellular matrix, cell surface structures including focal adhesions, interaction with neighboring cells, and the intracellular motile machinery including actin stress fiber and myosin reorganization (21-23). The small GTPases of the RHO family have been shown to play pivotal roles in these signal transduction pathways leading to cell migration and metastasis (24-26). In addition to RHO family members, several other signaling pathways have been identified to promote cell migration and invasion. Such pathways include ERK, CAS/CRK, PI3K-AKT pathway, and the low M(r) protein-tyrosine phosphatase (PTP) (27-34). In the present study, we overexpressed synuclein-γ in breast MDA-435 cells

Correspondence to: Dr Zhongzong Pan, Department of Animal Science, University of Vermont, 570 Main Street, Burlington, VT 05405, USA
E-mail: zpan@uvm.edu

Present address: [3]Health Technology Assessment Information Service, Plymouth Meeting, PA 19462, USA

Key words: synuclein-γ, cell motility, RHO, GTPase, ERK, breast cancer, ovarian cancer

and ovarian A2780 and OVCAR5 cells and evaluated its effect on the activity of the RHO family members. Our data indicate that both RHO and ERK are involved in synuclein-γ enhanced cell migration.

Materials and methods

Cell culture. Ovarian cancer cell lines A2780 and OVCAR5 were maintained in 10% FBS DMEM and 10% FBS RPMI-1640, respectively. Breast cancer cell line MDA-MB-435 (kindly provided by J.W. Liu) was maintained in 10% FBS DMEM/F12. Synuclein-γ overexpressing cells were derived by transfection and neomycin selection following the procedure as previously described (12). To knock-down synuclein-γ, OVCAR5 cells were transfected with siRNA duplex (Dharmacon Res. Inc.) and oligofectamine (Invitrogen) following the manufacturer's protocols. The sequences of duplex siRNA specific for γ-synuclein are as follows: 5'- GGA GAAUGUUGUACAGAGCUU-3' (sense strand), and 3'-UUCCUCUUACAACAUGUCUCG-5' (antisense strand). Synuclein-γ protein level can be dramatically suppressed after two-round transfection.

Assays for cell migration and invasion. Boyden chamber assay was used for cell migration and invasion assay. Cells ($3x10^5$) were placed into the upper chamber of Biocoat cell culture chambers (8-μm pore size) (Becton Dickinson, Bedford, MA). FBS medium (10%) was added to both upper and lower chambers. To evaluate the numbers of cells undergoing migration and invasion, cells on the surface of the upper chamber were removed by swiping with cotton swabs. After fixing and staining with Protocol Hema3 Staining Set (Biochemical Sci. Inc., Swedesboro, NJ), the cells on the surface of the bottom chamber were counted at magnification 10x10. The number of migration cells per field (at magnification 10x10) was the average of five independent fields counted for each chamber. Where indicated, a two-tailed Student's t-test was used to test for significance.

RHO/RAC/CDC42 activity assay. Cells at 70-80% confluence were washed twice with ice-cold DPBS before scraping with lysis buffer (Upstate, Lake Placid, NY) on ice. For RAC/CDC42 assay, the cells were lysed in 1X MLB (25 mM HEPES, pH 7.5, 150 mM NaCl, 1% Igepal CA-630, 10 mM $MgCl_2$, 1 mM EDTA, and 10% glycerol, 5 mM NaF, 1 mM Na_3VO_4) containing protease inhibitor cocktail (Roche, Indianapolis, IN). For RHO assay, cells were lysed in 1X RLB (50 mM Tris-HCl, pH 7.2; 500 mM NaCl; 10 mM $MgCl_2$, 0.5% sodium deoxycholate, 0.1% SDS, 5 mM NaF, 1 mM Na_3VO_4, 1 mM PMSF, 1% Triton X-100) with the protease inhibitor cocktail. Cellular debris was removed by centrifugation at 14,000 x g for 15 min at 4°C. Protein concentrations were determined using Bio-Rad DC protein assay reagents, and total cell lysate (1000 μg protein in 1 ml) was immunoprecipitated with either 10 μg PAK-1 PBD agarose (for RAC and CDC42) or 30 μg Rhotekin RBD agarose (for RHO) at 4°C for 1 h. After washing 3 times with lysis buffer, the pull-out GTP-bound RHO/RAC/CDC42 protein was eluted by boiling in SDS-sample buffer and evaluated by SDS-PAGE and immuno-blotting.

SDS-PAGE and immuno-blotting. For SDS-PAGE, proteins in the total cell lysate or eluted from agarose beads were separated on 4-20% linear gradient Tris-HCl ready gels (Bio-Rad), and transferred onto PVDF membranes (Millipore, Bedford, MA). Anti-ERK1 and anti-ERK2 antibodies were obtained from Santa Cruz Biotechnology, Inc. (Santa Cruz, CA). Anti-phospho-ERK1/2 was obtained from Cell Signaling Technology (Beverly, MA). γ-2 (gift from Dr B.I. Giasson) is a rabbit polyclonal antibody against synuclein-γ. The results of immuno-blotting were quantitated using the NIH Image for the integrated density of each band.

Results

Synuclein-γ overexpression enhanced cell migration in breast and ovarian cancer cells. The close correlation of synuclein-γ expression and breast and ovarian cancer staging suggests that synuclein-γ might be involved in advanced stage tumor progression and metastasis. Jia and colleagues showed that synuclein-γ overexpression in breast cancer cell line MDA-MB-435 cells enhanced cell motility *in vitro* and metastasis *in vivo* (19). To unravel the molecular mechanism by which synuclein-γ promotes cell motility, we overexpressed synuclein-γ in MDA-435 cells as well as the ovarian cancer cell lines A2780 and OVCAR5 cells (Fig. 1A). Consistent with a previous study by Jia *et al* (19), we observed that overexpression of synuclein-γ leads to elevated cell motility in MDA-MB-435 cells. Similarly, we observed that synuclein-γ overexpression leads to increased cell motility in ovarian cancer cell lines OVCAR5 and A2780 cells (Fig. 1). In Boyden chamber assay, overexpression of synuclein-γ enhanced cell motility in A2780 cells by 2- to 3-fold, OVCAR5 cells by 5- to 7 fold, and MDA435 cells by 3- to 4-fold (Fig. 1). These data indicate that synuclein-γ overexpression can enhance cell motility in both breast and ovarian cancer cells.

We further evaluated whether suppression of synuclein-γ has any effect on cell motility. OVCAR5 cells were used for this purpose because of the high endogenous synuclein-γ expression in this cell line. We found that cells treated with siRNA showed a significant decrease in the number of migration cells compared to untreated or mock-treated cells (data not shown). These data further support a role for synuclein-γ in cell motility.

Activation of the RHO and ERK pathways by synuclein-γ overexpression. Among the signaling molecules regulating cell motility, the small GTPases of the RHO family have been shown to play pivotal roles in these signal transduction pathways leading to metastasis (24-26,35). In support of the correlation of synuclein-γ with a motile cell phenotype, we found that the GTP-bound active form of at least one member of the RHO family GTPases is elevated in cells that overexpress synuclein-γ (Fig. 2). In MDA435/gam cells, activated RHO was increased about 3-fold by synuclein-γ. In OVCAR5/gam cells, RAC and CDC42 were activated by synuclein-γ, the level of activated RAC or CDC42 was increased approximately 2-fold. Interestingly, RHO, RAC, and CDC42 all showed a 2- to 3-fold increase of the active form in A2780/gam cells, although the fold increase in cell migration in A2780/gam cells was less than that of MDA435/gam and OVCAR5/gam cells.

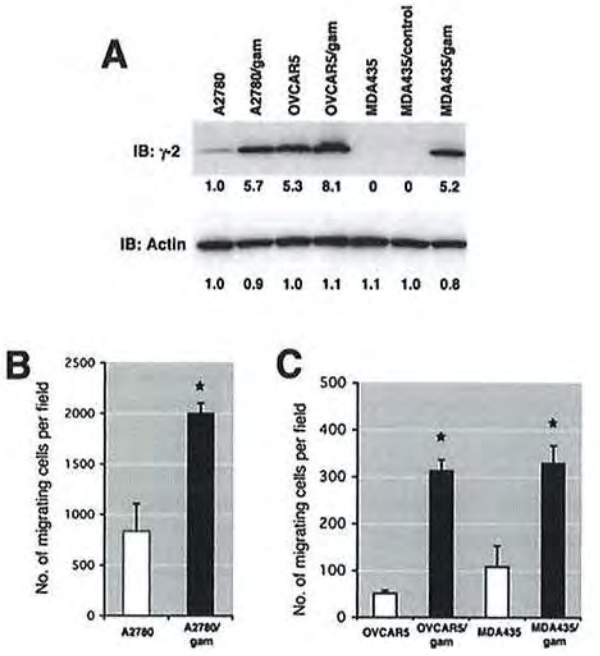

Figure 1. Synuclein-γ overexpression can enhance breast and ovarian cancer cell migration. (A) Synuclein-γ protein expression levels. Whole cell lysates from the parental cells or stably-transfected cells were analyzed by SDS-PAGE and immuno-blotting. Protein levels of synuclein-γ were determined by immuno-blotting (IB) with γ-2, a polyclonal antibody specific for synuclein-γ. Protein loading levels were evaluated by immuno-blotting with anti-actin antibody. The numbers beneath each band represent the densitometry units; A2780 was assigned an arbitrary unit of 1.0 for blots with γ-2 and actin, respectively. Shown here is a representative blot of three independent experiments. (B and C) Boyden chamber assay for cell migration and invasion. In Boyden chamber assay, $3x10^5$ cells were plated in the top chamber and cells migrating into the bottom chamber were fixed and stained at 48 h. Cells migrating into the bottom chamber were counted and shown in the graph are the means ± SEM of migrating cell number per field of triplicate chambers. Shown here is the representative of three independent experiments. *Significant difference ($p<0.05$) compared to the parental cells.

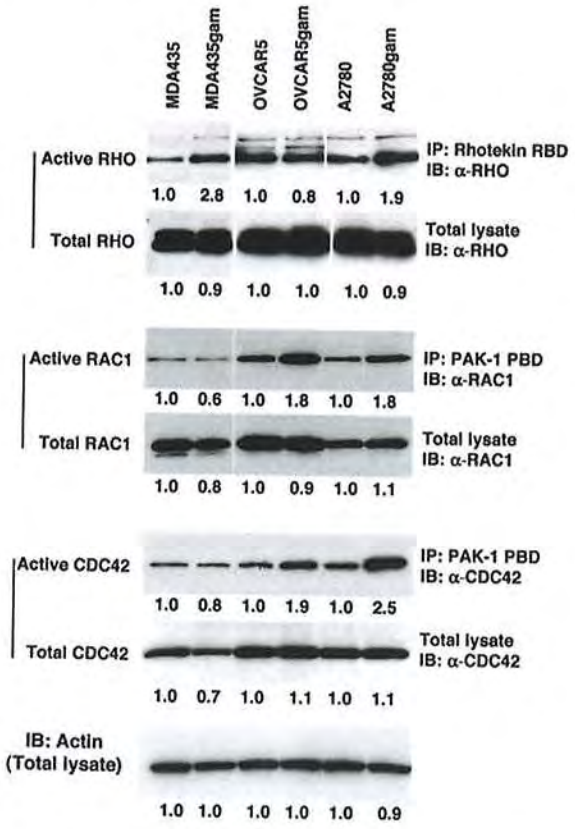

Figure 2. Activation of RHO family members by synuclein-γ overexpression. For RHO activation assay, total cell lysates (1500-2000 μg protein in 1 ml) from parental cells and their derivative cells that stably overexpress synuclein-γ were incubated with 30 μg Rhotekin RHO binding domain for 1 h at 4°C. Total RHO from 30 μg protein of whole cell lysate or the active GTP-bound RHO immunoprecipitated by Rhotekin RBD were detected by SDS-PAGE and immuno-blotting using a polyclonal antibody that recognizes RHO A, B, C. For RAC1 and CDC42 activation assay, total cell lysates (~1000 μg protein in 1 ml) from parental cells and their derivative cells that stably overexpress synuclein-γ were incubated with 15-20 μg PAK-1 PBD agarose for 1 h at 4°C. Total RAC1 or CDC42 from 30 μg protein of whole cell lysate or the active GTP-bound RAC1 or CDC42 immunoprecipitated by PAK-1 PBD were detected by SDS-PAGE and immuno-blotting using monoclonal antibodies that recognize RAC1 or CDC42, respectively. Protein loading levels were evaluated by immuno-blotting with anti-actin antibody. Experiments were performed three times and data from one representative assay are shown. The number beneath each band represents the arbitrary densitometry units of the corresponding band, and each of the parental cell lines (i.e., MDA435, OVCAR5, and A2780, respectively) was assigned an arbitrary unit of 1.0.

The reason we did not observe a more pronounced increase in cell motility in A2780/gam cells is not clear. Synucleins show low homology to 14-3-3 chaperone proteins and have been shown to have chaperone activity as analyzed *in vitro* (36,37), so we analyzed the protein levels of RHO, RAC, and CDC42 in total cell lysates but none of them was affected by synuclein-γ in any of these cell lines. These data indicate that the activation of RHO GTPase family members by synuclein-γ is not mediated by affecting the stability of the proteins.

As described previously, several other signaling pathways including ERK have also been identified to promote cell migration and invasion (27-34). In our previous study, we found that ERK is associated with and activated by synuclein-γ in A2780/gam and OVCAR5/gam cells (12). Similarly, we found that synuclein-γ overexpression led to an approximate 4-fold increase of ERK activation in MDA435/gam cells (Fig. 3). These data suggest that ERK might also be involved in synuclein-γ enhanced cell motility.

Both RHO and ERK pathways are required for synuclein-γ-enhanced cell motility. To determine whether the RHO pathway and ERK pathway are involved in synuclein-γ-enhanced cell motility, we evaluated the motility of cells treated with *C. difficile* Toxin B, an inhibitor for all RHO/RAC/CDC42 members (38), or with the MEK1 inhibitor U0126. The number of migration OVCAR5/gam cells treated with *C. difficile* Toxin B or U0126 was reduced 60-70% compared to untreated cells. The number of migration OVCAR5 cells treated with *C. difficile* Toxin B or U0126 was also reduced but to much less extent than OVCAR5/gam cells (Fig. 4A). The number of migration OVCAR5/gam cells treated with either inhibitor is still higher than the untreated parental OVCAR5 cells. In MDA435 and MDA435/gam cells, treatment with either *C. difficile* Toxin B or U0126 almost completely abrogated cell migration (Fig. 4B). *C. difficile* Toxin B or U0126 at the dosage used here did not affect cell viability (data not shown). These data further support the hypothesis that synuclein-γ-enhanced cell motility might be mediated by activation of RHO and ERK pathways.

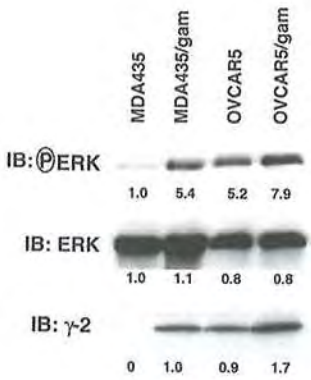

Figure 3. Activation of ERK by synuclein-γ overexpression. Total cell lysates from parental cells and their derivative cells that stably overexpress synuclein-γ were separated by SDS-PAGE and analyzed by immuno-blotting. Phosphorylated ERK was detected with phospho-ERK specific antibody, and total ERK1/2 was detected with antibodies recognizing total ERK1 and ERK2. The number beneath each band represents the arbitrary densitometry units of the corresponding band; MDA435 was assigned an arbitrary unit of 1.0 for blots with p-ERK and ERK, respectively; and MDA435/gam was assigned an arbitrary unit of 1.0 for blot with γ-2.

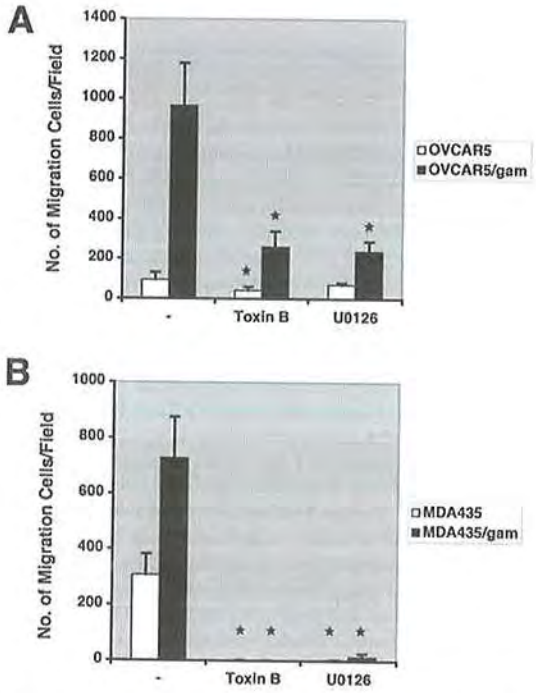

Figure 4. Requirement of RHO family members and ERK in cell migration. Cells ($3x10^5$) from parental or synuclein-γ overexpressing cells were plated in the top chamber in 10% FBS medium for Boyden chamber assay. After allowing cell attachment for 8 h (A) or 13 h (B), both the top and bottom chamber were replaced with 10% FBS medium containing 0.5 ng/ml *C. difficile* Toxin B (Sigma-Aldrich, St. Louis, MO), an inhibitor of RHO/RAC/CDC42, or 10 μM U0126 (Promega, Madison, WI), an inhibitor of MEK1/2. Cells migrating into the bottom chamber were counted at 66 h (A) or 52 h (B). The graphs represent the means ± SEM of migrating cell number per field of triplicate chambers. Experiments were repeated three times and data from one representative assay are shown. *Significant difference ($p<0.05$) compared to untreated cells.

Discussion

It has been well established that cancer cells contain many genetic and epigenetic alterations, some are bystander biomarkers, while others could be key etiologic factors contributing to tumor progression and metastasis. Our data in the present study provided further evidence supporting the role of synuclein-γ in cell migration and invasion. The mechanism by which synuclein-γ enhances cell motility is not clear. MMPs might be one of the mechanisms involved as MMP-2 and -9 are up-regulated by γ-synuclein in retinoblastoma Y79 cells (20). In MDA-MB-435 cells, however, ectopic overexpression of γ-synuclein did not activate MMPs (19), suggesting that this mechanism could be cell type dependent. The data in our present study indicated that the small G-protein RHO GTPases and ERK may be involved in synuclein-γ-enhanced cell motility in breast and ovarian cancer cells.

It remains to be determined how synuclein-γ leads to constitutively activated RHO family member(s). The activity of RHO family members is determined by the ratio of GTP/GDP-bound forms in the cells and the switch of these two forms is regulated by guanosine nucleotide exchange factors (GEFs), GTPase activating proteins (GAPs), and guanosine nucleotide dissociation inhibitors (GDIs) (39,40). One possible mechanism for synuclein-γ to activate RHO family members could be by regulating GEFs, GDIs, and GAPs involved in the GTP/GDP exchange, or by regulating signaling event(s) related to GDP/GTP exchange. The RHO family members may regulate different aspects of the cell motility machinery and there are cross-regulations among them depending on the cell type (39,41-44). The activation of RHO family members by synuclein-γ could be redundant or contribute to different aspects of cell motility and invasion.

In addition to the RHO pathway, we found that activation of ERK is also involved in synuclein-γ-enhanced cell motility. We observed in this study that serum is required for synuclein-γ-enhanced cell motility (data not shown), suggesting that ERK inactivation in serum-starved cells could be one of the reasons that cells lose their motile capacity in serum-free medium (12). The inhibitors for RHO family members and ERK inhibit the cell motility of both parental and synuclein-γ overexpressing cells, reflecting the fact that these proteins involved in normal cellular processes are not ideal cancer therapy targets. By detailing the mechanism of how RHO family members and ERK are activated by synuclein-γ, we might be able to abrogate the enhanced activation of these signaling proteins without affecting their normal function.

Acknowledgements

This work was supported in part by the Lake Champlain Cancer Research Organization (LCCRO), the Eileen Stein-Jacoby Fund, the Department of Defense (DAMD17-01-1-0522, DAMD17-03-1-0115), and NCI Ovarian Cancer SPORE P50 CA83638. We thank Dr Jingwen Liu for providing the MDA-MB-435 cells, and Dr Benoit Giasson for providing the γ-2 anti-serum.

References

1. Lavedan C: The synuclein family. Genome Res 8: 871-880, 1998.
2. Surguchov A, Surguchev, I, Solessio E and Baehr W: Synoretin - a new protein belonging to the synuclein family. Mol Cell Neurosci 13: 95-103, 1999.

3. Clayton DF and George JM: Synucleins in synaptic plasticity and neurodegenerative disorders. J Neurosci Res 58: 120-129, 1999.
4. Ji H, Liu YE, Jia T, *et al*: Identification of a breast cancer-specific gene, BCSG1, by direct differential cDNA sequencing. Cancer Res 57: 759-764, 1997.
5. Bruening W, Giasson BI, Klein-Szanto AJ, Lee VM, Trojanowski JQ and Godwin AK: Synucleins are expressed in the majority of breast and ovarian carcinomas and in pre-neoplastic lesions of the ovary. Cancer 88: 2154-2163, 2000.
6. Surgucheva I, McMahan B, Ahmed F, Tomarev S, Wax MB and Surguchov A: Synucleins in glaucoma: implication of gamma-synuclein in glaucomatous alterations in the optic nerve. J Neurosci Res 68: 97-106, 2002.
7. Celis A, Rasmussen HH, Celis P, *et al*: Short-term culturing of low-grade superficial bladder transitional cell carcinomas leads to changes in the expression levels of several proteins involved in key cellular activities. Electrophoresis 20: 355-361, 1999.
8. Sinha P, Hutter G, Kottgen E, Dietel M, Schadendorf D and Lage H: Search for novel proteins involved in the development of chemoresistance in colorectal cancer and fibrosarcoma cells *in vitro* using two-dimensional electrophoresis, mass spectrometry and microsequencing. Electrophoresis 20: 2961-2969, 1999.
9. Fung KM, Rorke LB, Giasson B, Lee VM and Trojanowski JQ: Expression of alpha-, beta- and gamma-synuclein in glial tumors and medulloblastomas. Acta Neuropathol 106: 167-175, 2003.
10. Liu H, Liu W, Wu Y, *et al*: Loss of epigenetic control of synuclein-gamma gene as a molecular indicator of metastasis in a wide range of human cancers. Cancer Res 65: 7635-7643, 2005.
11. Gupta A, Godwin AK, Vanderveer L, Lu A and Liu J: Hypomethylation of the synuclein gamma gene CpG island promotes its aberrant expression in breast carcinoma and ovarian carcinoma. Cancer Res 63: 664-673, 2003.
12. Pan ZZ, Bruening W, Giasson BI, Lee VM and Godwin AK: Gamma-synuclein promotes cancer cell survival and inhibits stress- and chemotherapy drug-induced apoptosis by modulating MAPK pathways. J Biol Chem 277: 35050-35060, 2002.
13. Gupta A, Inaba S, Wong OK, Fang G and Liu J: Breast cancer-specific gene 1 interacts with the mitotic checkpoint kinase BubR1. Oncogene 22: 7593-7599, 2003.
14. Liu J, Spence MJ, Zhang YL, Jiang Y, Liu YE and Shi YE: Transcriptional suppression of synuclein gamma (SNCG) expression in human breast cancer cells by the growth inhibitory cytokine oncostatin M. Breast Cancer Res Treat 62: 99-107, 2000.
15. Lu A, Zhang F, Gupta A and Liu J: Blockade of AP1 transactivation abrogates the abnormal expression of breast cancer-specific gene 1 in breast cancer cells. J Biol Chem 277: 31364-31372, 2002.
16. Inaba S, Li C, Shi YE, Song DQ, Jiang JD and Liu J: Synuclein gamma inhibits the mitotic checkpoint function and promotes chromosomal instability of breast cancer cells. Breast Cancer Res Treat 94: 25-35, 2005.
17. Jiang Y, Liu YE, Goldberg ID and Shi YE: Gamma synuclein, a novel heat-shock protein-associated chaperone, stimulates ligand-dependent estrogen receptor alpha signaling and mammary tumorigenesis. Cancer Res 64: 4539-4546, 2004.
18. Jiang Y, Liu YE, Lu A, *et al*: Stimulation of estrogen receptor signaling by gamma synuclein. Cancer Res 63: 3899-3903, 2003.
19. Jia T, Liu YE, Liu J and Shi YE: Stimulation of breast cancer invasion and metastasis by synuclein gamma. Cancer Res 59: 742-747, 1999.
20. Surgucheva IG, Sivak JM, Fini ME, Palazzo RE and Surguchov AP: Effect of gamma-synuclein overexpression on matrix metalloproteinases in retinoblastoma Y79 cells. Arch Biochem Biophys 410: 167-176, 2003.
21. Orr FW and Wang HH: Tumor cell interactions with the microvasculature: a rate-limiting step in metastasis. Surg Oncol Clin North Am 10: 357-381, 2001.
22. Orr FW, Wang HH, Lafrenie RM, Scherbarth S and Nance DM: Interactions between cancer cells and the endothelium in metastasis. J Pathol 190: 310-329, 2000.
23. Turley EA: Molecular mechanisms of cell motility. Cancer Metastasis Rev 11: 1-3, 1992.
24. Etienne-Manneville S and Hall A: Rho GTPases in cell biology. Nature 420: 629-635, 2002.
25. Clark EA, Golub TR, Lander ES and Hynes RO: Genomic analysis of metastasis reveals an essential role for RhoC. Nature 406: 532-535, 2000.
26. Ridley AJ: Rho GTPases and cell migration. J Cell Sci 114: 2713-2722, 2001.
27. Klemke RL, Cai S, Giannini AL, Gallagher PJ, De Lanerolle P and Cheresh DA: Regulation of cell motility by mitogen-activated protein kinase. J Cell Biol 137: 481-492, 1997.
28. Krueger JS, Keshamouni VG, Atanaskova N and Reddy KB: Temporal and quantitative regulation of mitogen-activated protein kinase (MAPK) modulates cell motility and invasion. Oncogene 20: 4209-4218, 2001.
29. Cho SY and Klemke RL: Extracellular-regulated kinase activation and CAS/Crk coupling regulate cell migration and suppress apoptosis during invasion of the extracellular matrix. J Cell Biol 149: 223-236, 2000.
30. Anand-Apte B, Zetter BR, Viswanathan A, *et al*: Platelet-derived growth factor and fibronectin-stimulated migration are differentially regulated by the Rac and extracellular signal-regulated kinase pathways. J Biol Chem 272: 30688-30692, 1997.
31. Delehedde M, Sergeant N, Lyon M, Rudland PS and Fernig DG: Hepatocyte growth factor/scatter factor stimulates migration of rat mammary fibroblasts through both mitogen-activated protein kinase and phosphatidylinositol 3-kinase/Akt pathways. Eur J Biochem 268: 4423-4429, 2001.
32. Ellerbroek SM, Halbleib JM, Benavidez M, *et al*: Phosphatidylinositol 3-kinase activity in epidermal growth factor-stimulated matrix metalloproteinase-9 production and cell surface association. Cancer Res 61: 1855-1861, 2001.
33. Wicki A and Niggli V: The Rho/Rho-kinase and the phosphatidylinositol 3-kinase pathways are essential for spontaneous locomotion of Walker 256 carcinosarcoma cells. Int J Cancer 91: 763-771, 2001.
34. Chiarugi P, Cirri P, Taddei L, *et al*: The low M(r) protein-tyrosine phosphatase is involved in Rho-mediated cytoskeleton rearrangement after integrin and platelet-derived growth factor stimulation. J Biol Chem 275: 4640-4646, 2000.
35. Ridley AJ: Rho family proteins: coordinating cell responses. Trends Cell Biol 11: 471-477, 2001.
36. Ostrerova N, Petrucelli L, Farrer M, *et al*: alpha-Synuclein shares physical and functional homology with 14-3-3 proteins. J Neurosci 19: 5782-5791, 1999.
37. Souza JM, Giasson BI, Lee VM and Ischiropoulos H: Chaperone-like activity of synucleins. FEBS Lett 474: 116-119, 2000.
38. Bishop AL and Hall A: Rho GTPases and their effector proteins. Biochem J 348: 241-255, 2000.
39. Van Aelst L and D'Souza-Schorey C: Rho GTPases and signaling networks. Genes Dev 11: 2295-2322, 1997.
40. Takai Y, Sasaki T and Matozaki T: Small GTP-binding proteins. Physiol Rev 81: 153-208, 2001.
41. Guasch RM, Scambler P, Jones GE and Ridley AJ: RhoE regulates actin cytoskeleton organization and cell migration. Mol Cell Biol 18: 4761-4771, 1998.
42. Banyard J, Anand-Apte B, Symons M and Zetter BR: Motility and invasion are differentially modulated by Rho family GTPases. Oncogene 19: 580-591, 2000.
43. Sander EE, ten Klooster JP, van Delft S, van der Kammen RA and Collard JG: Rac downregulates Rho activity: reciprocal balance between both GTPases determines cellular morphology and migratory behavior. J Cell Biol 147: 1009-1022, 1999.
44. Spaargaren M and Bos JL: Rab5 induces Rac-independent lamellipodia formation and cell migration. Mol Biol Cell 10: 3239-3250, 1999.